The Comprehensive Roadmap Toward Malaria Elimination Using Graphene and its Promising 2D Analogs

Fangzhou He, George Junior, Rajashree Konar, Yuanding Huang, Ke Zhang, Lijing Ke, Meng Niu, Boon Tong Goh, Amine El Moutaouakil, Gilbert Daniel Nessim, Mohamed Belmoubarik,* and Weng Kung Peng*

Malaria is a major public health concern with over 200 million new cases annually, resulting in significant financial costs. Preventive measures and diagnostic remedies are crucial in saving lives from malaria, and especially in developing nations. 2D materials are, therefore, ideal for fighting such an epidemic. Graphene and its derivatives are extensively studied due to their exceptional properties in this case. The biomedical applications of graphene-based nanomaterials have gained significant interest in recent years due to their remarkable biocompatibility, solubility, and selectivity. Their unique physicochemical characteristics, like ample surface area, biofunctionality, high purity, solubility, substantial drug-loading capacity, and superior ability to penetrate cell membranes, make them up-and-coming candidates as biodelivery carriers. In this review, crucial graphene-based technologies to combat malaria are discussed. The advancements in preventing and diagnosing malaria and the biocompatibility of graphene-based nanomaterials are emphasized. The roadmap for using graphene-based technology toward achieving the WHO global malaria elimination by 2030 is presented and discussed in detail. Graphene oxide, the most critical biocompatible graphene derivative for health sensors, is also discussed. Additionally, 2D chalcogenides, specifically sulfide-based transition-metal dichalcogenides, are reviewed in detecting malaria during its early stages.

1. Introduction

In 2022, there were ≈249 million malaria cases, resulting in a death toll of 608 000. This highlights the significant impact of malaria as a prominent public health issue.[1] Malaria is a serious health concern that needs to be diagnosed and treated promptly. Adopting a two-stage approach to diagnosis and prevention is essential to combat this disease. By doing so, we can effectively reduce the incidence and mortality rates associated with malaria and work toward eradicating malaria epidemics by 2030.[2] In alignment with the WHO program, the Lancet Commission recognizes the crucial importance of malaria elimination and has set a target of achieving this goal by 2050. To realize this objective, the commission emphasizes the utilization of innovative and robust technologies.[3] Specifically, rapid diagnostic tests (RDTs) will play a crucial role in accurately identifying malaria infections,

F. He, Y. Huang, K. Zhang, W. K. Peng
Frontier Research Center
Songshan Lake Materials Laboratory
Dongguan 523-808, China
E-mail: pengwengkung@sslab.org.cn

G. Junior, M. Belmoubarik, W. K. Peng
Department of Quantum and Energy Materials
International Iberian Nanotechnology Laboratory
Braga 4715-330, Portugal

R. Konar, G. D. Nessim
Department of Chemistry
Bar-Ilan Institute of Nanotechnology and Advanced Materials
Bar-Ilan University
Ramat Gan 5290002, Israel

The ORCID identification number(s) for the author(s) of this article can be found under https://doi.org/10.1002/anbr.202300130.

L. Ke
School of Food Science and Nutrition
University of Leeds
Leeds LS2 9JT, UK

M. Niu
Department of Interventional Radiology
Shengjing Hospital of China Medical University
Shenyang 110001, China

B. T. Goh
Low Dimensional Materials Research Centre (LDMRC)
Department of Physics
Faculty of Science
University of Malaya
Kuala Lumpur 50603, Malaysia

A. E. Moutaouakil
Department of Electrical and Communication Engineering
United Arab Emirates University
P.O. Box 15551, Al Ain, United Arab Emirates

M. Belmoubarik
Institute of Applied Physics
Mohammed VI Polytechnic University
Lot 660, Hay Moulay Rachid Ben Guerir 43150, Morocco
E-mail: mohamed.belmoubarik@um6p.ma

enabling prompt treatment and control measures. Artemisinin-based combination therapy, known for its high efficacy against malaria parasites, will also serve as a cornerstone of effective treatment strategies. Additionally, deploying long-lasting insecticide-treated nets (LLINs) will help to prevent mosquito bites and minimize disease transmission.

Malaria eradication is a vital investment and offers substantial social and economic reward through the eradication dividend. In the absence of eradication, the constant risk of importation and resurgence necessitates ongoing investments in surveillance and periodic, intense interventions to manage outbreaks that are bound to occur. The ramifications of a substantial malaria resurgence, which could result in significant mortality rates among nonimmune groups, underscore the catastrophic effects that can be prevented through intentional and continuous measures.

In recent times, several categories of malaria detection technologies have emerged. They include targeting *Plasmodium falciparum* histidine-rich protein 2 (PfHRP-2), parasite lactate dehydrogenase (PLDH), aldolase, glutamate dehydrogenase (GDH), the biocrystal hemozoin, and biomolecules such as DNA and proteins;[4–7] the emergence of point of care;[4,8–12] and wearable technologies[13–17] (detection limit: $\approx$50 parasite μL^{-1}).[13] The current diagnostic tools available for malaria are constrained in their sensitivity, accuracy, and applicability, particularly in settings where resources are limited.[18,19] Effective detection and diagnosis of malaria cases are hindered by certain limitations, which impede timely treatment and control efforts. Emerging 2D materials, such as tungsten diselenide (WSe$_2$),[20] black phosphorus,[21] and MXenes,[22] show potential in malaria diagnosis.

However, low sensitivity, weak stability, complex manufacturing, and limited biocompatibility are some issues that need to be handled in this class of 2D materials. This is why, in recent years, we have focused on graphene-based devices as promising tools for diagnosing and treating several diseases, including anemia,[23] jaundice,[24] and malaria.[25,26]

Graphene is a 2D nanomaterial of carbon atoms arranged in a hexagonal lattice. This material exhibits exceptional physical characteristics, including remarkable mechanical, electrical, optical, and thermal properties. It is also notable for its high transparency, biocompatibility, chemical stability, and thermoelectric properties. Moreover, it is relatively inexpensive to produce and easy to fabricate, making it a promising material for many applications. These include the development of inks, fabrics, electronics, sensors, communication devices, and biomedical tools. Graphene-based devices have been shown to improve the sensitivity, selectivity, and accuracy of diagnostic tests for malaria and the efficacy of antimalarial drugs[27] (**Figure 1** and **Table 1**). The study conducted by Zamzam et al.[28] presented a graphene-based polarization-insensitive metamaterial, demonstrating its potential for susceptible and accurate detection of malaria infection in various biosensing applications with a sensitivity of 2.538 THz RIU^{-1}.

Our review article explores the use of graphene and related 2D materials in sensing applications for rapid malaria diagnosis. These technological advancements have the potential to reduce and manage malaria transmission significantly. Research and exploration into the development of graphene-based devices have proven invaluable in enhancing our understanding of the
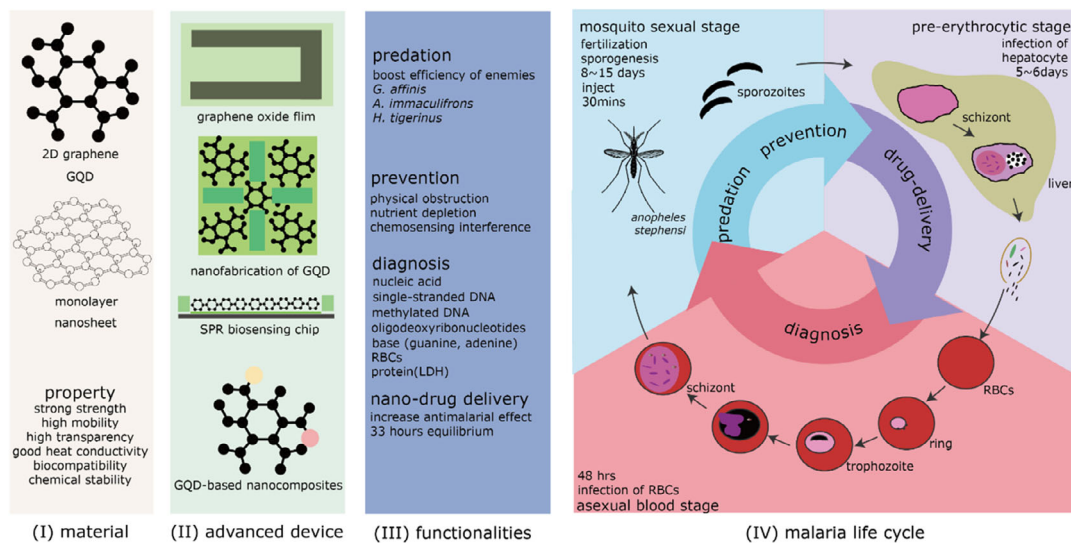

Figure 1. Graphene in the fight against malaria. I) Material based on a diversity of graphene (e.g., 0D, 1D, 2D, 3D, monolayer, multilayer, and nanosheet) with chemical properties of strong strength, high mobility, high transparency, good heat conductivity, biocompatibility, and chemical stability; II) advanced devices (e.g., nanofabrication of graphene quantum dots, surface plasmon resonance biosensing chip) demonstrating antimalarial characteristics can be used for III) malaria treatment (i.e., enhanced predation efficiency of natural enemies, prevented *P. falciparum* bites by acting as physical barrier, interference *P. falciparum* sense the human body, the superior loading capacity of graphene oxide nanosheets (GOns) for essential biomolecules required for the growth and development of malaria parasites resulted in the depletion of vital nutrients, diagnosis malaria by rapid detection of DNA, RBC, lactate dehydrogenase (LDH), and nanodrug delivery system with high toxicity against malaria mosquitoes) at IV) different stages of malaria development from injection of sporozoites by an infected mosquito to multiplication of merozoites in RBCs. This review contributes to a better understanding of the opportunities and challenges associated with graphene-based materials in the fight against malaria, offering valuable guidance for future research and development in this important area.

Table 1. Recent advances in graphene-based devices for prevention and diagnosis of malaria.

Function	Device	Type	Target analyte	Limit of detection	References
Prevention	Graphene oxide nanosheet	Nanosheet	*Plasmodium falciparum*	Not related	Kenry (2017)
Prevention	Graphene-based film	Film	Mosquito bite	Not related	Castilho (2019)
Predation	Graphene quantum dots	Quantum dot	*Anopheles stephensi*	Not related	Murugan (2016)
Diagnosis	Aptamer-graphene oxide biosensor	Multilayer	*Plasmodium falciparum* LDH	0.5 fM	Jain (2016)
Diagnosis	Field-effect transistor-based biosensors	Monolayer	DNA/RNA	600 zM (≈18 molecules)	Hwang (2020)
Diagnosis	Plasmonic sensor	Monolayer	RBCs	4.7 THz RIU^{-1}	Nejat (2019)
Diagnosis	Plasmon resonance biosensor	Multilayer	Malaria-specific oligodeoxyribonucleotides	12 pM	Wu (2020)
Diagnosis	Surface plasmon resonance biosensor	Nanofilm	RBCs	258.28° RIU^{-1}	Uniyal (2022)
Diagnosis	Surface plasmon resonance biosensor	Multilayer	RBCs	240.10° RIU^{-1}	Panda (2022)
Diagnosis	Quantitative electrical biosensor	Multilayer	*Plasmodium falciparum* LDH	0.11 pg mL^{-1}	Figueroa-Miranda (2022)
Diagnosis	Graphene-based nanosensor	Monolayer	RBCs	840 nm RIU^{-1}	Seyyedmasoumian (2022)
Diagnosis	Sensor kit	Nanoparticles	RBCs	40 vivax-infected RBCs/10 μl blood	Singh (2021)
Nano-drug delivery	Nanocomposites	Quantum dot	Parasitemia	Not related	Torkashvand (2023)

potential applications and challenges graphene-based materials face in the battle against malaria.[6,11,29–31] This is expected to advance the roadmap for using graphene-based technology to achieve the WHO goal of eliminating malaria globally by 2030 (**Figure 2**). In addition to graphene-based devices, we have also dedicated a section to understanding the biocompatibility and issues related to analogous 2D materials such as sulfide-based transition-metal dichalcogenides (TMDCs) in malaria detection.

2. Characteristics of Graphene as a Versatile 2D Material

Graphene is an ultrathin 2D material with exceptional mechanical, electronic, and thermal properties, making it promising for a wide range of applications in various fields of science and technology (bond length 1.42 Å). Its unique honeycomb lattice structure gives it exceptional microstructural properties (**Figure 3**).[32,33] In 2004, Professor Andre Geim and Professor Konstantin Novoselov exfoliated few-layer graphene (FLG) from graphite using the famous scotch tape method. This ingenious breakthrough has since made graphene a promising candidate for various fields, despite its zero-bandgap value.[34] Initially, research on graphene focused on its superior properties compared to the commonly used silicon material in modern electronics. However, its potential as a versatile material has been increasingly emphasized, with applications ranging from inks and flexible electronics to fabrics.[35] In addition to its cost-effectiveness and ease of synthesis, and due to its many unique and fascinating properties, graphene, as well as graphene-based devices, covered a variety of applications such as communication, electronics, spintronics, and medical applications to replace widely used nanomaterials (i.e., silicon and compound semiconductors).[36–50] Posing a noteworthy benefit, the charge carriers within graphene can be viewed as massless relativistic particles or Dirac fermions. This phenomenon arises from the closure of both valence and conduction bands at the corners

of the Brillouin zone (so-called zero bandgap), leading to a linear dispersion of the energy spectrum.[51]

Interestingly, the metallike property can be changed to semiconducting by forming graphene nanoribbons (GNRs) with controllable size. It has been verified that GNRs with dimensions less than 10 nm exhibit semiconducting properties owing to the quantum confinement effect.[52] However, for larger widths, these properties are significantly influenced by the edge configurations.[53] While Geim and Novoselov's exfoliated graphene from graphite using scotch tape is not scalable,[54] chemical vapor deposition (CVD) synthesis of graphene, though well established, yields too low quantities (one sheet on the substrate), making it suitable for specific electronic or sensor applications rather than large-scale production. As a practical alternative, we can explore the viability of graphene oxide (GO), which can be produced in larger quantities.

At room temperature, graphene displays an anomalous half-integer quantum Hall effect that applies to both electrons and holes.[55] Also, owing to the delocalized p bonds in the out-of-plane resulting from the sp^2 hybridization of intercarbon atoms, substantial electrical conductivity is observed (mobility of charge carriers ≈200 000 cm^2 V^{-1} s^{-1}).[56] In addition, it also has some other unique properties like substantial specific surface area (≈2630 m^2 g^{-1}), remarkable mechanical strength (nearly 200 times stronger than steel with Young's modulus ≈1100 Gpa), excellent thermal conductivity (≈5000 Wm^{-1} K^{-1}), and electrical conductivity exceeding 1000 Sm^{-1}.[57] All these properties are for the monocrystalline graphene, referred to as pristine graphene.

Graphene is often used in barrier coatings and membranes due to its barrier properties against gases, liquids, small molecules, and mosquito bites.[58,59] The distinctive composition and characteristics of the material allow it to function as a highly effective shield against a range of environmental factors, thus rendering it a highly valuable substance for protective purposes. The exceptional biocompatibility, functional versatility, and hydrophilic properties of graphene and GO render them highly appealing materials for various medical and bioapplications.
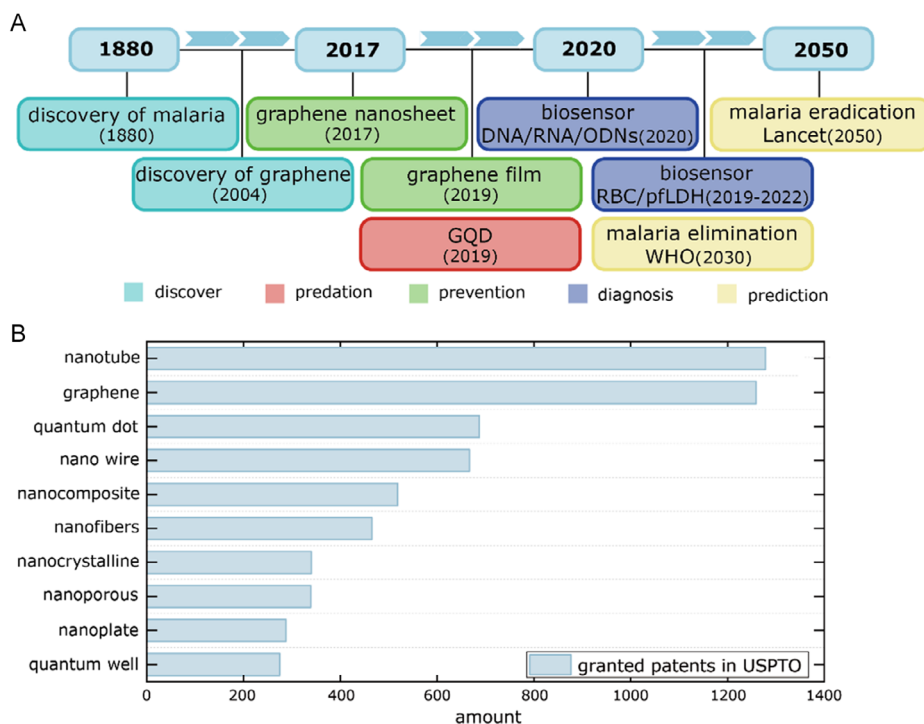
Figure 2. Critical milestones in discovering, predating, preventing, diagnosing, and predicting malaria and graphene-based antimalaria technologies. A) In 1880, the discovery of malaria marked a significant milestone in understanding this infectious disease. Graphene, a groundbreaking material, was first isolated and characterized by Andre Geim and Konstantin Novoselov at the University of Manchester in 2004. Multiple graphene-based films and nanosheets have recently been developed to prevent malaria and the interference of pathogen sensing (2017–2022). In late 2020, biosensors utilizing DNA, RNA, ODNs, etc., were developed for rapid and precise malaria detection; WHO has set a program for malaria elimination by 2030, encompassing a range of strategic interventions aimed at reducing the incidence and burden of malaria, improving access to prevention and treatment measures, strengthening surveillance, and monitoring systems, and fostering international collaborations. The Lancet Commission has acknowledged the significance of malaria elimination. It has established a target of attaining this objective by 2050 through the implementation of innovative and robust technologies, including rapid diagnostic tests (RDTs), artemisinin-based combination therapy (ACT), and long-lasting insecticide-treated nets (LLINs). B) Nanomaterials have the highest number of granted patents in the United States Patent and Trademark Office (USPTO).

Integrating these graphene-based materials into biosensor modules presents a compelling opportunity to enhance the detection and monitoring of specific analytes while offering a protective barrier. Incorporating graphene and its derivatives in biosensor systems offers unprecedented opportunities for improving the speed and sensitivity of analyte detection (**Figure 4**). The distinct physicochemical attributes of graphene, including its elevated surface-to-volume ratio, excellent electrical conductivity, and biocompatibility, enable efficient signal transduction and enhance the performance of biosensors. Moreover, the hydrophilic nature of graphene allows for effective biomolecular immobilization and promotes specific interactions between the target analytes and the sensor surface.

The exceptional mechanical strength and impermeability of graphene provide a robust and reliable protective layer, ensuring the integrity and longevity of the biosensor system. This barrier function is particularly crucial in applications where the sensor needs to operate in complex biological environments or in the presence of interfering substances. Integrating graphene and its derivatives into biosensor modules enhances the ability to detect analytes with higher sensitivity and selectivity, enhancing the overall performance[60,61] and longevity[62] of the biosensor. So, graphene and its 2D analogs possess exceptional properties

and multifunctional capabilities, making them highly versatile for developing advanced biosensing platforms. These platforms will eventually enable improved detection and tracking of specific analytes, making them ideal for medical and bioapplications, especially considering their shielding properties.

Graphene offers the benefit of producing various graphene-derivative materials by synthesizing them on different substrates and surfaces through diverse methods. This versatile ability amplifies the potential of graphene for tailored applications. Graphene stands out as a distinctive type of carbon allotrope, serving as the foundational unit for all other carbon allotropes. Its remarkable properties enable it to be stacked to create 3D graphite and rolled into the shape of 1D nanotubes (carbon nanotubes [CNTs]).[63] All chemical derivatives derived from graphene, including GO, reduced GO (rGO), FLG, fluorographene, hydrogenated graphene (HG), wrinkled graphene, rGO hybridized with nanoparticles (NPs), graphene nanopore (GNP), GNR, nano-sized GO, commonly referred to as graphene quantum dots (GQDs), etc. (Figure 3A), are considered valuable components and applicable constituents for biosensors, real-time bioimaging, cancer diagnosis and treatment, catalysis, water purification, etc.[64–67] Graphene biosensing's features for viral infection have been thoroughly reported in the literature.[42,68,69]
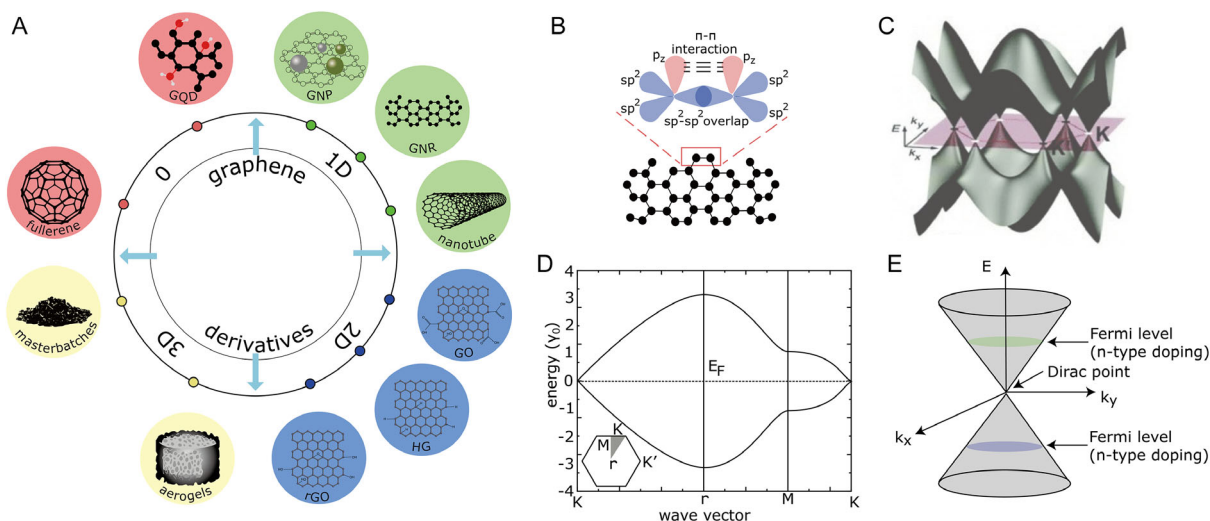
Figure 3. Schematic of structures and states of graphene and its derivatives. A) Graphene materials can be categorized based on different dimensions: 0D (fullerene and GQD), 1D (carbon nanotube [rolled graphene], GNP, and GNR), 2D (GO, rGO, and HG), 3D (graphene-based aerogels and graphene masterbatches). B) The chemical structures of pristine graphene are composed of pure-arranged carbon atoms with sp^2-hybridized carbon atoms. The distribution of delocalized π electrons on the graphene surface enables strong hydrophobic interactions and π–π stacking interactions with various molecules. Further, it enhances the binding affinity that results from the overlap of π orbitals between graphene and the aromatic rings of the therapeutic molecules. C) The 3D band structure of graphene. The symmetry characteristic of graphene band structure allows for reducing these six neutrality points into a pair known as K and K′ that are independent of one another, meaning that the electronic behavior around K does not affect the behavior around K′ and vice versa. D) Dispersion of the states of graphene. E) The low energy band structure is approximated as two cones touching at the Dirac point. The position of the Fermi level determines the nature of the doping and the transport carrier. Adapted under the terms of the CC BY 4.0 licence.[69] Copyright 2017, The Authors. Published by MDPI; Adapted under the terms of the CC BY 4.0 licence.[187] Copyright 2022, The Authors. Published by Elsevier; and Adapted under the terms of the CC BY 4.0 licence.[188] Copyright 2010, The Authors. Published by American Chemical Society.
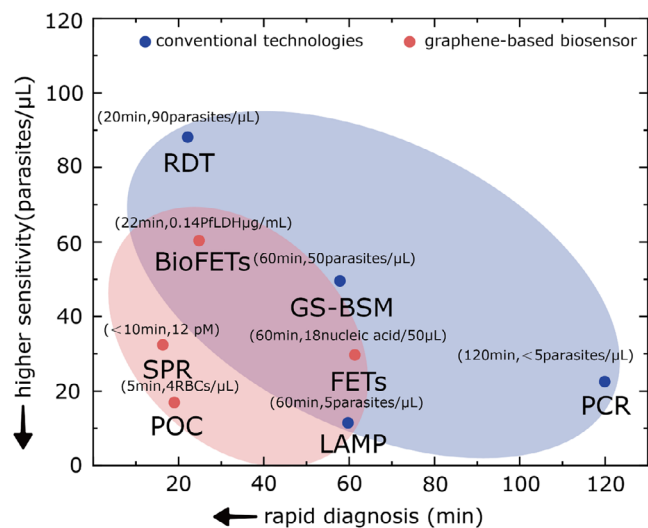

Figure 4. Biparametric map of comparison of conventional technology. Rapid diagnostic test (RDT), genome-sequencing-based blood stage malaria (GS-BSM), loop-mediated isothermal amplification (LAMP), polymerase chain reaction (PCR), and graphene-based technology (SPR, BioFET, FET, Point-of-Care [POC]) on sensitivity level and diagnostic efficiency.

3. Synthesis of Graphene and Its Derivatives

Graphene can be synthesized via two approaches: the top-down and bottom-up synthesis routes. The top-down approach involves exfoliation or cleavage of a carbon source such as graphite or carbon CNTs. This can be achieved through mechanical exfoliation using scotch tape, liquid-phase exfoliation, oxidative exfoliation, GO reduction, CNTs unzipping, and arc discharge. The oxidative exfoliation and reduction of GO can be done through chemical reduction, thermal reduction, or electrochemical reduction methods. In contrast, the bottom-up synthesis of graphene includes CVD, epitaxial growth on substrates such as SiC, template-based synthesis, or total organic synthesis. A detailed schematic containing information on different synthesis routes of graphene and its analogs is presented in **Figure 6**A–H.

The mechanical exfoliation method is a simple and repeatable process that can produce monolayers or multilayers of high-quality graphene. This has been confirmed through evaluations using Raman, atomic force microscopy, and optical microscope techniques, all while keeping production costs low. Nonetheless, a constraint of this approach is its impact on scalability due to the direct influence of yield. The procedure depends on generating sheer force to surpass van der Waals attraction and create graphene layers. The liquid-phase exfoliation technique is an efficient chemical detachment process to separate the graphene layers from bulk graphite without causing extreme fragmentation effects.[71] It operates by inducing high-speed shock waves by controlling the power, medium, and frequency. This method can be effectively scaled up by addressing technical needs like

Yet, it is believed that it can serve in both the prevention and the biosensing of parasitic diseases such as malaria (**Figure 5**) due to its high stretchability, total flexibility, yet high impermeability, chemical inertness, and intrinsic biocompatibility.[7,33,37,70]
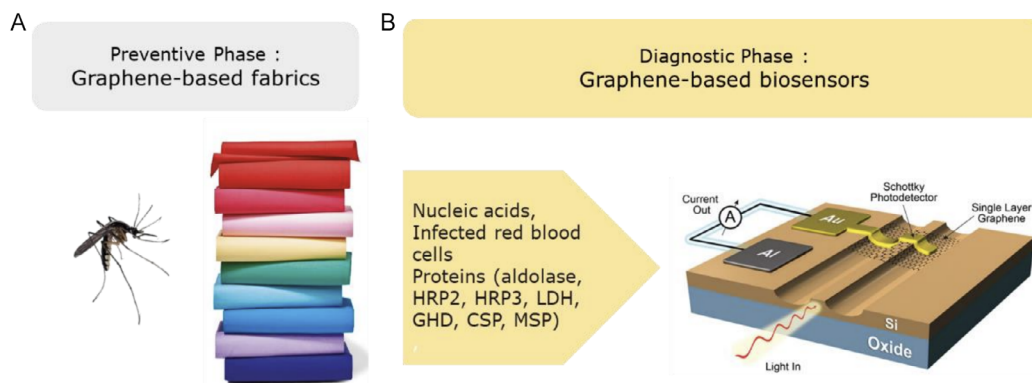
Figure 5. The applications of graphene-based materials in the A) preventive and B) diagnostic phases against malaria. (A) Graphene-based films are used as barriers in fabrics, which can interfere with the chemosensing. This form of "molecular barrier" prevents mosquitoes from detecting skin-associated molecular attractants encrusting beneath the graphene films. In addition, graphene-based films also deter mosquitoes from penetrating biological barriers due to their exceptional barrier properties against gases, liquids, small molecules, and mosquito bites. (B) Graphene-based biosensors are developed to detect the presence of parasites (e.g., DNA) or the host biomolecule markers (e.g., proteins). Key-enabling technologies of graphene in the fight against malaria are classified into different categories, that is, targeting *Plasmodium falciparum* histidine-rich protein 2 (PfHRP-2), parasite lactate dehydrogenase (PLDH), aldolase, glutamate dehydrogenase (GDH), the biocrystal hemozoin, and biomolecules (e.g., DNA and proteins)[4–7], and emergence point-of-care technologies, that is, graphene-related nanosheet-based sensors, microneedle patch, graphene-based film, quantitative electrical biosensor, with sensitive detection limits and fast detection speed.[59,166,184,185] Adapted under the terms of the CC BY 4.0 licence.[189] Copyright 2016, The Authors. Published by American Chemical Society.

power efficiency, source distribution, and a larger vessel to make it more suitable for industrial applications. In one study, Huang et al.[72] introduced a two-step process that can enhance and homogenize the bonding strength among the outermost layers of graphene sheets and the multilayer graphite by introducing a substrate and controlling the forces between the loaded crystal layer(s) and the substrate.

The electrochemical method of wet chemical exfoliation is an effective way of producing a significant amount of graphene.[73] This process involves the application of voltage to drive the ion toward the graphite electrode, leading to the formation of gaseous molecules that intercalate and force the exfoliation process. Chemical exfoliation is the most efficient method for producing high-quality graphene on a large scale. Mechanical exfoliation methods have shown promising results, but their scalability is limited due to the requirement of high-pressure vessels for jet milling.[74] In contrast, chemical methods such as electrochemical exfoliation show great promise. Combining electrochemical and sonication methods allows graphene size to be regulated by adjusting factors such as reaction duration, power input, and temperature.

The CVD synthesis route uses gaseous carbon precursors such as ethylene and methane instead of graphite as the carbon source. A transition-metal-containing substrate is exposed to these hydrocarbon precursors at high temperatures within furnaces. The generated graphene possesses an extensive surface area, presenting it as a potential material for energy-related applications. However, this method's drawbacks include high production costs, low output, and the need for a purification method to remove the residue catalyst used during CVD.[75] Despite these drawbacks, this method is better than others as it produces a large quantity of pristine graphene. The metal's carbon solubility affects the outcome of graphene produced, with low-carbon solubility metals forming nucleation sites on the metal catalyst surface.[76]

High-carbon solubility metals diffuse the carbon precursor on the heated metal surface, forming graphene sheets around the metal surface. A chemical etching process detaches graphene layers from the metal substrate[76] to transfer graphene from the metal surface. Although an extra step, this method is easy and not too complicated in creating high-quality graphene layers. Sun et al.[77] reported a detailed study for growing misorientation-free graphene domains on Cu (111) foils in the nucleation stage.

Furthermore, graphene and its derivatives are effective in detecting malaria. This is because the number of layers in graphene affects its sensing mechanism. Mono- to multilayer graphene exhibits heightened sensitivity and finds application in sensor technologies, capable of detecting biomolecules, elements, gas, pressure, and electrochemical activity. Owing to its expansive surface area, electrical conductivity, biocompatibility, user-friendly operation, adjustable structural transformation, and exceptional mechanical strength, layered graphene has gained popularity in biomedical devices. It has proven effective in detecting bacteria and viruses and facilitating regenerative drug delivery. Graphene is an excellent substrate for studying biomolecules that contain hydrophobic regions. This is because molecules such as DNA and proteins tend to naturally adsorb onto the surface of graphene, making it easy to modify and use for further analysis.[78] Another practical approach to tailor graphene to immobilize bioreceptor units with precision is introducing functionalization using Au or Ag nanoparticles. This technique has shown promising results and is widely adopted due to its simplicity and efficacy.

In contrast, GO is generally synthesized using Hummers' method or derivative from where the graphene layer contains covalent links such as hydroxyl (—OH), carboxylic acid (—COOH), carbonyl (C—O), alkoxy (C—O—C), and other oxygen groups. The method mainly consists of making a chemical reaction using graphite in a solution, in most common solutions such as $KMnO_4$. The surface may be treated by acquiring a

**ADVANCED
SCIENCE NEWS**

www.advancedsciencenews.com

**ADVANCED
NANOBIOMED
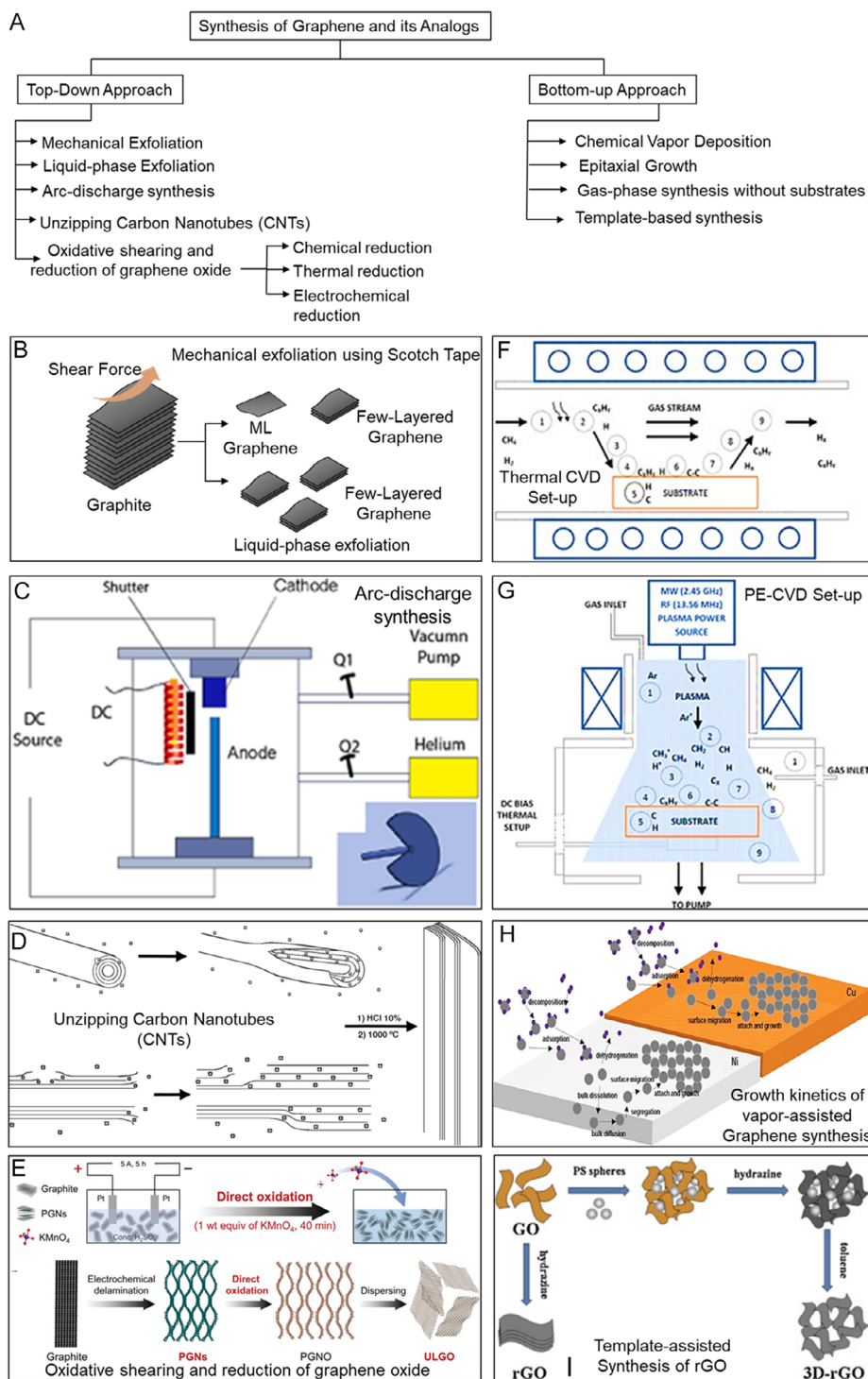RESEARCH**
Open Access

www.advnanobiomedres.com

Figure 6. Schematic showing the synthesis of graphene and its analogs. A) Schematic showing the different routes of graphene (and its analogs) synthesis via top-down and bottom-up approaches. B) Exfoliation route to synthesize graphene either mechanically or via ultrasonication in low-boiling solvents. C) Arc-discharge setup details to produce graphene on a large scale. D) Carbon nanotubes (CNTs) can be easily unzipped by longitudinally intercalating Li/NH$_3$ followed by exfoliation. E) The process described oxidative shearing and reduction of graphene oxide (GO), where ultralarge graphene oxide (ULGO) was prepared in one-pot synthesis, including electrochemical delamination and the subsequent oxidative exfoliation. Furnace setups for F) thermal chemical vapor deposition (CVD) and G) plasma-enhanced chemical vapor deposition. H) Growth kinetics of graphene in the bottom-up CVD synthesis on Ni and Cu substrate using CH$_4$ as the carbon source. I) Template-assisted synthesis of reduced graphene oxide (rGO). Adapted under the terms of the CC BY 4.0 licence.[190–194] Copyright 2015, The Authors. Published by IOP; Copyright 2009, The Authors. Published by American Chemical Society; Copyright 2022, The Authors. Published by Wiley; Copyright 2013, The Authors. Published by Wiley; and Copyright 2014, The Authors. Published by Elsevier.

**ADVANCED
SCIENCE NEWS**

www.advancedsciencenews.com

**ADVANCED
NANOBIOMED
RESEARCH**
Open Access

www.advnanobiomedres.com

reduction of bodies of oxygen groups, which makes a reduced GO. The last kind of oxidized graphene uses the edge of the graphene and is optimized using GQD.

The synthesis is defined to block the dangling bonds derivative from graphite exfoliation. The large-scale area can be done with a centrifuge machine using graphite and oxidants.[79] The material can get sizes around 30–500 μm in an average reaction for 3 h. The treatment of the graphene planar zone can be improved by removing the excessive oxidized radicals that block the link with nonpolar interaction. This reduction is called reduced rGO. The chemical reaction is known as an electrochemical reduction by potential electrodes.

The GO's properties differ from the graphene pristine, where the sp^2 link is broken for oxidation, which changes the current–voltage (I–V) curve for biosensors. This change increases the graphene resistance to $40\,Sm^{-1}$ and rGO to $200\,Sm^{-1}$.[80] The properties are high since they differ from the unoxidized pristine graphene, where the Young Modules go to 207 GPa. GO or rGO reduces the electric properties. However, they offer the advantage of being more cost-effective,[80] capable of large-scale production,[73] and having better biosensor biocompatibility and hydrophobicity.

Another distinguishing property of graphene is its electrochemical reactivity. CVD-synthesized graphene is highly resistant to various oxidizing chemicals, making it an ideal material for many applications. Moreover, this type of graphene can be easily transferred through electrolysis, facilitating its use in various fields.[81] It is possible to selectively target the analyte through chemically precise functionalization, paving the path for the creation of biosensors. Since foreign molecules can access the entire surface area of graphene, it is considered a highly favorable nanoplatform for detecting adsorbed molecules with a high adsorption capability.[82] As previously described, several functionalization techniques may make it very selective for capturing specific molecules. Graphene has a significant advantage over nanomaterials like CNT due to its lack of impurities postsynthesis. Usually, impurities within CNTs retain electrochemical activity, posing potential toxicological hazards and diminishing their sensitivity and selectivity. In contrast, graphene's homogeneous composition ensures it remains a safe and reliable option for various applications.[83,84]

4. Biocompatibility and Toxicity of Graphene and Its Derivatives

When considering using any nanomaterial in biological applications, it is vital to evaluate its biosafety in cells and living organisms based on various physiological parameters like adsorption, distribution, metabolism, excretion, and toxicity. This raises the question of whether graphene is biocompatible and offers advantages over other nanomaterials. Recent research has highlighted graphene's potential in biomedical areas, including improved cell growth and differentiation, cancer treatment through DNA sequencing, biosensing, therapeutics, drug delivery, stem cell research, tissue engineering, and more.[85] The compatibility of graphene and its derivatives with biological systems is contingent upon factors such as their lateral size, dosage, functionalization, charge, and reactive oxygen species (ROS), as indicated by

in vivo toxicity studies.[86–88] The liver, lungs, spleen, and kidneys are the most common sites for GO buildup. Researchers found that GO can be promptly cleaned from the bloodstream and that buildup in the liver can be eliminated via liver secretion into the bile tract system.[89,90] Yet, because of the enormous size (1–5 μm) and 2D structure of GO, it is difficult for the kidneys and lungs to filter it out, whereas the liver[83] retains smaller sizes (110–500 nm). Many additional studies have found that GO purification by multiple washing stages, polymeric modifications (such as PEGylation is a biochemical modification process of bioactive molecules with polyethylene glycol (PEG) graphene), and conjugation techniques via surface modifications improve biocompatibility and circulation times in vivo.[91,92] Moreover, the genotoxicity of graphene, GO, and rGO has been somewhat explored. Carbon equivalents like single-walled carbon nanotube and C60 have demonstrated cytotoxicity, genotoxicity, and ROS production.[93] Bengtsan et al.[94] found that rGO with lateral dimension >1 nm did not produce genotoxicity or ROS formation in FE1 murine lung epithelial cells in vitro. In contrast, research in in vivo conditions is strongly advised to understand the biological impacts completely. Before conferring the status of "biosafe" on graphene and its derivatives, it is imperative to evaluate many factors carefully. These include size distribution, the quantity of oxygen-containing groups (directly influenced by the production method), optimal dosage, the tendency for aggregation formation, surface coating, and other relevant considerations.[95,96]

The reduced particle size of graphene and its derivatives increases their surface area, resulting in an enhanced ability to penetrate biological barriers, thereby increasing the potential for toxicity. Excessive amounts of oxygen-containing groups in graphene and its derivatives can lead to increased cytotoxicity, primarily determined by the method of production[97,98] (**Figure 7**). Optimum dosage is critical for both therapeutic efficacy and cellular damage. The appropriate dosage of a material is a crucial factor that affects its therapeutic efficacy and potential cellular damage. Excessive exposure to a material may result in cellular damage, while insufficient dosages may not produce the intended therapeutic effect.[99] Aggregation formation tendency can reduce therapeutic efficacy by making it difficult for cells to uptake these materials.[100] Coating graphene and its derivatives with biocompatible materials can enhance their biocompatibility and reduce toxicity.[101] Thus, properly controlling and regulating these factors are essential for ensuring the safe use of graphene and its derivatives in biomedical applications. Several studies have investigated these factors, including the work of Majeed et al.[102] focusing on particle-size-based toxicity in graphene, and the survey by Jastrzębska et al.[103] focusing on the effect of the synthesis method on the biocompatibility of GO.

5. Graphene in Malaria Elimination: Preventative Phase

5.1. Preventative Phase: Graphene-Based Nanomaterials in Fabrics

Mosquitoes track humans from more than 50 m, ascribed to their developed senses of thermal signatures and visual and olfactory signals.[104] Humans can, therefore, be detected by their
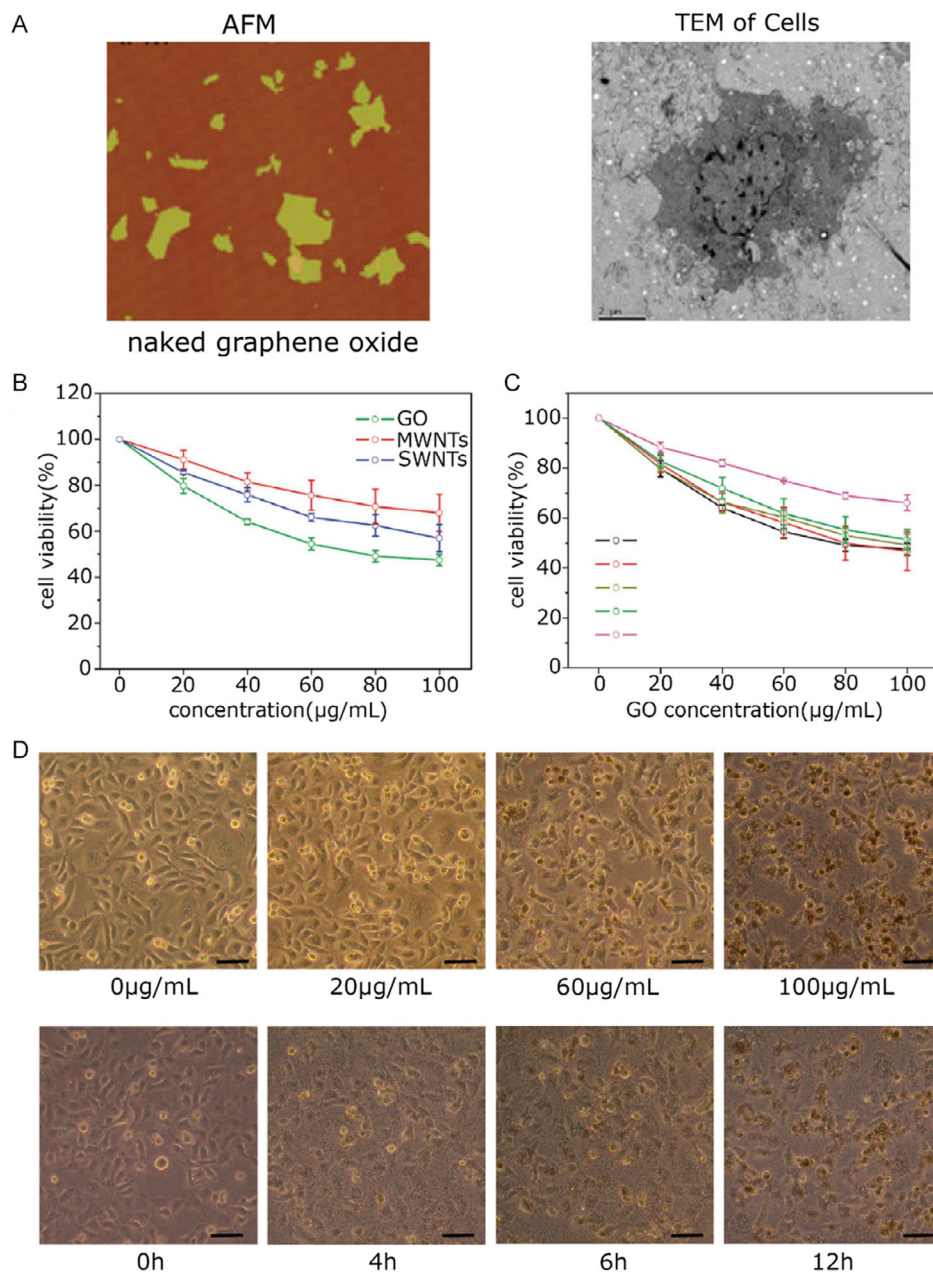
**ADVANCED
SCIENCE NEWS**

www.advancedsciencenews.com

**ADVANCED
NANOBIOMED
RESEARCH**

www.advnanobiomedres.com

Figure 7. Cytotoxicity assessment of GO nanosheets against A549 cells in complete RPMI 1640 medium supplemented with 10% v/v FBS. A) Cytotoxicity of GO nanosheets is attributed to direct interactions between the cell membrane and GO nanosheets, leading to physical damage to the cell membrane. B) The cytotoxic effects of 100 µg mL^{-1} carbon nanotubes (multi-walled and single-walled) were compared with GO nanosheets on A549 cells after 24 h, as determined by MTT (3-(4, 5-dimethylthiazolyl-2)-2, 5-diphenyltetrazolium bromide) assays. C) The viability of A549 cells was assessed after treatment with different concentrations of GO nanosheets and varying incubation times. D) Morphological alterations in A549 cells were observed after exposure to different concentrations of GO nanosheets for 24 h (top), as well as following treatment with 100 µg mL^{-1} GO nanosheets over a series of incubation times (bottom) with a scale bar of 20 µm. Adapted under the terms of the CC BY 4.0 licence.[97] Copyright 2011, The Authors. Published by American Chemical Society.

skin-associated molecular attractants, such as water vapor, CO_2, and skin microbiota metabolites. *Plasmodium falciparum* (*P. falciparum*) malaria parasites produce volatile compounds, including terpenes, which resemble plants. These compounds serve as interspecies chemical signals, or semiochemicals, influencing the attraction of vector mosquitoes toward hosts.[105]

Approaches on how to hide these attractants are fundamental to the prevention of malaria.

Traditionally, the prevention against malaria is predominantly based on LLINs, considered one of the main vector-control strategies backed by the WHO and Lancet committee.[3,106] In high-risk areas, the population, especially women and children under

5 years old, is recommended to sleep under LLINs to reduce the chances of mosquito bites. Other preventive strategies include chemoprevention—through ingesting drugs against infections—insecticide-treated nets (ITNs), and indoor residual spraying (IRS). However, ITN and IRS have shown limited efficiency overtime due to the resistance of parasites to the chemicals used.[107] The limited use of LLINs during rest/sleep time leaves the population vulnerable to mosquito bites during the rest of the day.

Given the complex and varied detection methods mosquitoes employ, a robust camouflaging solution appears to be the most effective means of mitigating viral contamination. Graphene multilayer films, in contrast, can serve as a physical barrier to mosquito bites as well as a molecular barrier to conceal the skin-associated molecular attractants, attributed to their solid 2D structures and their ability to withstand penetration forces of more than 50 µN in the case of 0.5 µm thick GO films (**Figure 8**).[59] Castilho et al.[59] showed that wearable technologies with embedded graphene-based films yield excellent results in protecting against mosquito bites as physical and molecular barriers. Dry GO and rGO films can interfere with the host-sensing system in mosquitoes, especially *Aedes aegypti*, by concealing the skin attractants. In wet rGO films, where a mosquito attractant was introduced intentionally, 0.5 µm thick graphene films showed sufficient mechanical puncture resistance against bite protection. Despite their lower biting frequency compared to cheesecloth, wet GO films were easily penetrated by mosquito bites due to their hygroscopic nature, making them easy to absorb water and swell and easily destroyed during handling.

The aforementioned works show that graphene can prevent malaria in several aspects. First, integrating graphene-based films into wearable technologies can decrease the frequency and chances of mosquito bites during all-day outings and activities. Combined with the lowered cost of graphene production, its nontoxicity, flexibility, and ease of synthesis, it provides an additional, if not an alternative, layer of protection to the widely used LLINs.

Other than clothing and LLIN-like nets with graphene-based materials, the use of graphene-based coating on the walls of housings in mosquitoes-populated areas can provide large-scale protection to the inhabitants against mosquito bites, as this will serve as a chemical barrier and as a camouflage to the CO_2 plume produced by the residents, and thus deprive mosquitoes of one of their long-distance sensing weapons. This alone will reduce the density of mosquitoes inside the housing premises, providing a guaranteed reduction in the spread of malaria.

5.2. Preventative Phase: Graphene-Based Nanomaterials in the Bloodstream

In addition to the wearable technologies, using graphene-based materials directly in the human bloodstream showed barrier-like behavior. With its hydrophilic nature, GO is more suitable for bioapplications than the hydrophobic pristine graphene. In vitro experiments[29] investigating the interactions between GO and *P. falciparum* concentrations indicate that GO nanosheets can effectively function as a physical barrier between red blood cells (RBCs) and the parasite. The parasite's merozoites could not access healthy RBCs due to their adhesion to GO nanosheets. The growth of the parasites from the ring to the trophozoite stage was hindered, and the presence of GO postponed their maturation. The strong affinity of GO toward various biomolecules, including the nutrients required for parasite growth, was demonstrated by its electrostatic and π–π interactions. A reduction in the viability of the parasites evidenced the antimalarial activity of GO. Other than GOs, GQDs showed excellent chemical and physical properties for biomedical applications and their toxicity against *P. falciparum*, both CQ-resistant and CQ-sensitive strains, *Plasmodium Berghei*, and young instars of malaria mosquitoes were demonstrated.[108] The GQDs also showed toxicity against Michigan Cancer Foundation (MCF)-7 breast cancer cell.[108] This result clearly shows the potential of GO and other graphene-based nanomaterials in preventing the proliferation of malaria parasites in the bloodstream and inhibiting their development into advanced stages, which opens the way for developing new nanomaterial-based approaches for fighting malaria.

In some cases, however, the attachment of GO to human cells may lead to adverse effects.[109] The number of in vivo studies is steadily increasing; a study demonstrated that GOs at doses below 20 µg mL^{-1} showed no observable toxic effects, while doses exceeding 50 µg mL^{-1} induced cytotoxicity through a decrease in cell adhesion and initiation of cell apoptosis.[89] The authors associated this cytotoxicity with the penetration of GOs into lysosomes, mitochondria, endoplasm, and the cell nucleus.[89] GO influences alveolar macrophages and alveolar epithelial cells by inducing the generation of ROS, resulting in inflammation and apoptosis of mitochondrial respiration.[110]

Furthermore, dose-dependent pulmonary toxicity, peribronchiolar lung fibrosis, and inflammatory cell infiltration have been observed following GO administration.[110] In a study, pristine graphene and GO accumulation induced multiorgan toxicity in zebra fish larvae or juveniles, leading to degeneration in brain and cardiac functions, hepatic damage, and neural impairment.[111] Similarly, administration of GO in mice has been shown to induce chronic toxicity and result in lung granuloma formation, leading to mortality.[89]

5.3. Bioimpact of Graphene-Based Nanomaterials on Humans

While the toxicity and bioimpact of graphene-based materials were discussed in several literature,[59,112] they remain unresolved concerns in integrating graphene-based nanomaterials in the prevention solution against malaria. Despite the rapid development of this technology, there are growing concerns regarding the leaching of graphene from products during use or disposal and its potential impact on the environment. While moderate fitness trackers and embedded electronic devices in clothes have been developed, as well as biocompatible coatings on body implants, the ecological toxicity of graphene on various organisms, including animals, plants, bacteria, and fungi, is becoming an increasing concern.[99,113,114] Yet, the potential impact of these nanomaterials on humans and the environment is still lacking data, especially in vivo, due to the shortage of robust and validated approaches for toxicology testing,[37] which will make the prediction of toxicity based solely on the material properties.
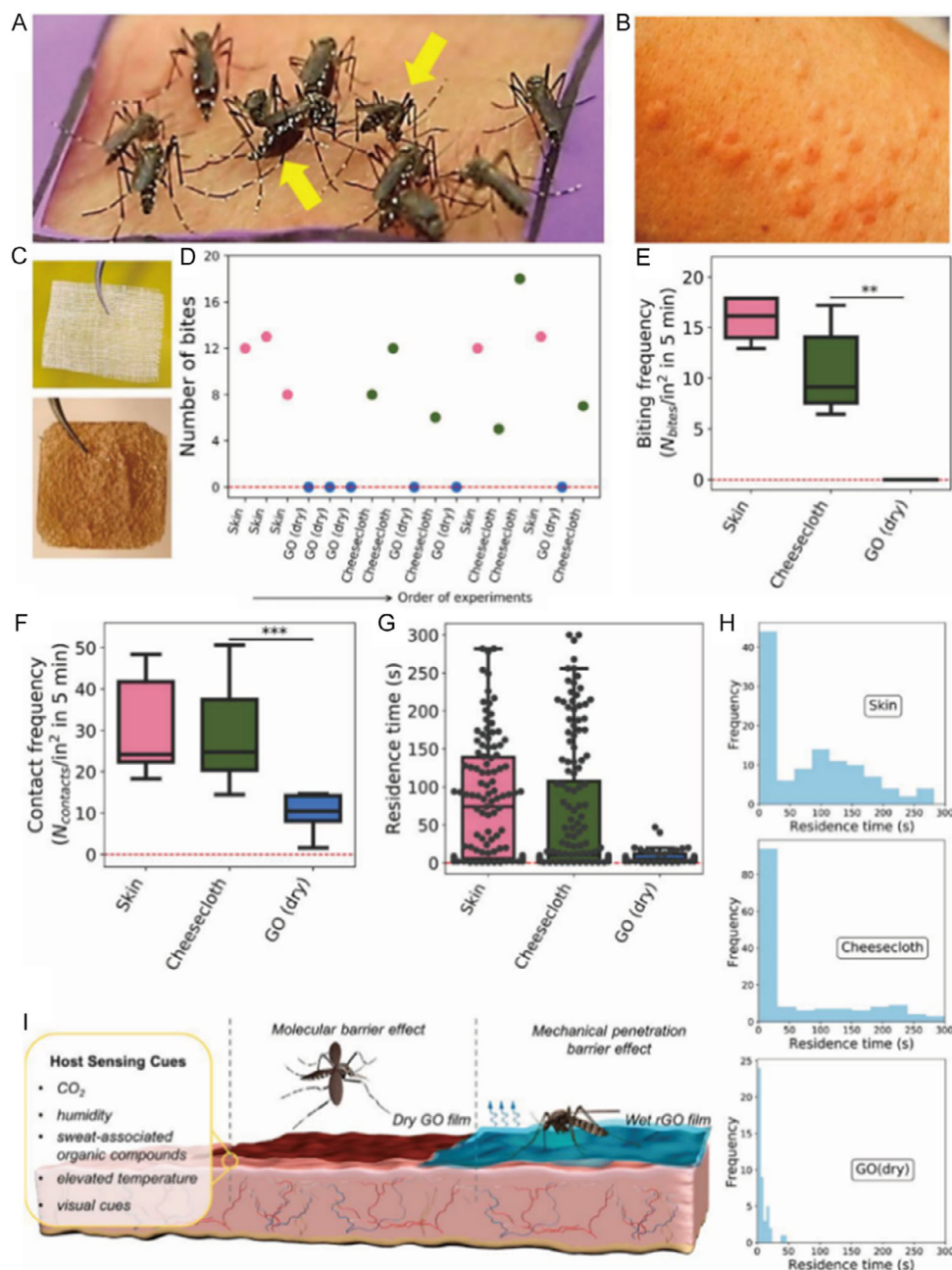
ADVANCED
SCIENCE NEWS

www.advancedsciencenews.com

ADVANCED
NANOBIOMED
RESEARCH
Open Access

www.advnanobiomedres.com

Figure 8. Analysis of the influence of graphene films in the dry state on mosquito biting behavior and the mechanisms involved in inhibiting mosquito bites. A) Illustration of typical Aedes mosquito behavior observed during control experiments on bare skin, with yellow arrows indicating two bite indicators: the left arrow shows a red and swollen abdomen, indicating successful blood feeding, while the right arrow shows a head-down position, indicating fascicle insertion. B) Image of a skin patch after a control experiment (without graphene), demonstrating the inflammatory reaction as a third bite indicator. C) Comparison of the structures of standard cheesecloth (top) and a GO nanosheet film with a 2 cm lateral dimension (bottom). D) Example raw data on bite counts (number of bites per 5 min experiment) presented in the order of randomized trials. No bites were recorded during any experiment with dry GO films. E) Box plot showing the frequency of mosquito bites normalized by the area on dry GO films compared to controls. F) Box plot showing the frequency of mosquito contacts (landings plus walk-ons) on dry GO films compared to controls. G) Box plot showing the residence times of Aedes mosquitoes after initial contact with dry GO films compared to controls (black circles represent individual data points). H) Residence time distributions (10 bins) of mosquitoes on skin, cheesecloth, and dry GO. I) Diagram illustrating possible mechanisms of bite inhibition on dry GO films and wet reduced rGO films. On the left, a selection of chemical, thermal, and optical cues reported to play a role in mosquito host sensing. The chemical cues, such as CO_2, humidity, and sweat-associated organic compounds, are rendered nonbioavailable by the molecular barrier effect exerted by the overlaying nonwetted GO films in the center. Adding water or sweat as an attractant on the outer surface of rGO films successfully attracts mosquitoes on the right but still prevents biting through a mechanical penetration barrier effect. Adapted under the terms of the CC BY 4.0 licence.[59] Copyright 2019, The Authors. Published by PNAS.

**ADVANCED
SCIENCE NEWS**

www.advancedsciencenews.com

**ADVANCED
NANOBIOMED
RESEARCH**
Open Access

www.advnanobiomedres.com

Direct exposure to graphene poses a certain level of risk and hazard. First, oral or ingestion of graphene derivatives is typically an intentional route, primarily when graphene and its derivatives are used as carriers for biologically active agents. However, accidental ingestion of graphene may occur in occupational settings, environmental exposure, and medical applications. A study investigating the exposure of graphene nanoplatelets showed that GO treatment resulted in a short-term decrease in mouse locomotor activity and neuromuscular coordination, resulting in mild fatigue.[115] Second, inhalation is another major route of human exposure in the long term. Inhalation of high concentrations of GO results in the accumulation of graphene in the lungs that persists for up to 90 days, causing acute pulmonary cell damage, pulmonary lesions, and neutrophil infiltration.[116] Finally, skin exposure is a vital medium and the most common route for wearable devices. Contact with graphene can cause skin diseases such as contact dermatitis, oxidative stress, and excessive keratinization, leading to skin toxicity.[117] There are limited toxicological data at the skin level, while most are in vitro studies on skin fibroblasts and keratinocytes depending on different derivatives. The graphene, for instance, was found to induce higher cytotoxicity on skin fibroblasts than GO due to the material aggregation,[118] while all graphene-based materials induced significant cytotoxicity on human keratinocytes with different potencies based on the oxidative state of the materials.[119]

The only available in vivo investigation showed that the GO injected into the dermis of the growing feather sites of chickens initiated an immune response after dermal injection.[120] From 3 days onward, clear aggregates of the injected graphene-based material could be observed and appeared to be inside cells or part of the build-up of cells inside and around the nanomaterial (**Figure 9**). Based on the literature, GOs have been reported to display dose- and size-dependent toxicity on various cell lines, such as human hepatocellular carcinoma, human fibroblasts, and human skin keratinocytes, etc.[89,121,122] Considering that GO-based drug delivery systems (DDSs) come into contact with cells and tissues, it is essential to understand their interaction with biological components despite the incomplete understanding of GO's behavior within the human body. Nano-sized GO at a concentration of $25 \, \mu g \, mL^{-1}$ displayed significant hemolysis (around 70%), while micro-sized GO sheets induced much lower hemolysis (≈10%) at $100 \, \mu g \, mL^{-1}$.[118] The size and surface modification of GO largely influences the interaction between GO and RBCs. Coating GO with specific agents such as chitosan, L-cysteine, and heparin results in the coverage of the interacting layer, reducing toxicity.[123]

Nevertheless, the integration of graphene-based materials in wearable technologies is less invasive compared to the mentioned studies due to the absence of direct contact with body cells. Still, skin irritation is the most logical outcome after cutaneous exposure.[37] This can be solved using graphene derivatives as inner fabric layers rather than on the surface to suppress dermal contact. A recent study has demonstrated the successful development of electrically heated textiles by employing graphene/poly(-vinylidene fluoride-co-hexafluoropropylene) composites as the base material for the inner layers of clothing and gloves, aimed at regulating body temperature.[124] In addition, GO-based nanomaterials have emerged as promising topical antimicrobial agents for use in cotton fabrics,[125] bandages, and ointments.[126]

Animal studies have shown that these materials are well tolerated and do not cause skin irritation. For example, Zhao et al.[127] synthesized a non-irritating antimicrobial agent based on cotton GO. At the same time, Xu et al.[128] investigated the dermal toxicity of silver-reduced GO on rat skin and found no evidence of skin irritation. However, limited information is available on the dermal toxicity of GO, and further studies are required to understand the underlying toxicological mechanism fully.

6. Graphene-Based Biosensors for Malaria Elimination

In the absence of appropriate preventive measures, early-stage diagnosis of malaria is considered a key element in the fight against malaria, as it can prevent transmission, reduce the draining of the available resources, minimize the unnecessary use of drugs, avoid the spread of life-threatening side effects, as well as the spread of drug resistance among the population.[129] Current diagnostics mainly use antigen-based RDTs, which have a short shelf life and are less sensitive than thick blood films. Detection methods need to be efficient, easy to deploy, cost-effective, and simple to operate to help fight malaria. Graphene-based biosensors are promising candidates for electrochemical detection and new generation point-of-care testing attributed to the graphene electrical and optical properties.[30,31,130] A real-time, label-free, highly sensitive, and inexpensive graphene-enhanced surface plasmon resonance (SPR) sensor conjugated with malaria-specific biomarker, oligodeoxyribonucleotides, is reported for malaria diagnosis and was able to complete the process in mere minutes.[131] Another SPR-based biosensor, with dual nanofilms of gold and graphene, has also been reported to diagnose severe malaria of various stages by measuring the refractive index (RI) alterations in RBCs.[132]

The advanced electrical and optical properties of graphene have been exploited in many fields.[32,33,133,134] One area attractive for graphene biosensing is the disposable screen-printed electrodes, where using the less performant multi-wall carbon nanotubes (MWCNTs) showed excellent results: 96% sensitivity and 94% specificity.[135] Assimilating graphene-based materials instead of MWCNTs will provide better sensitivity and higher signal-to-noise ratios than the reported sensor. In addition, the flexibility of the graphene paves the way for the graphene-based electrodes to be printed on other graphene-based flexible substrates and integrated on printed-circuit boards, making them commercially viable for malaria biosensors for clinical applications.

In addition, graphene-based sensors can integrate both the RDT and thick blood films owing to their ability to monitor the electronic transfer reactions of hemoglobin concentration, thus checking for the existence of malaria-caused anaemia.[30,31] The iron ion inside the hemoglobin can be in Fe^{II} or Fe^{III} oxidation states; the latter, which can be caused by malaria, hinders methemoglobin from binding to oxygen, resulting in fatality in the absence of internal reduction mechanisms within the RBCs. Toh, R.J. et al.[30] showed that it is possible to make direct in vivo electrochemical detection of hemoglobin in RBCs on glassy carbon electrodes using Nafion (**Figure 10** and **11**). This study confirms that the multifaceted biological conditions
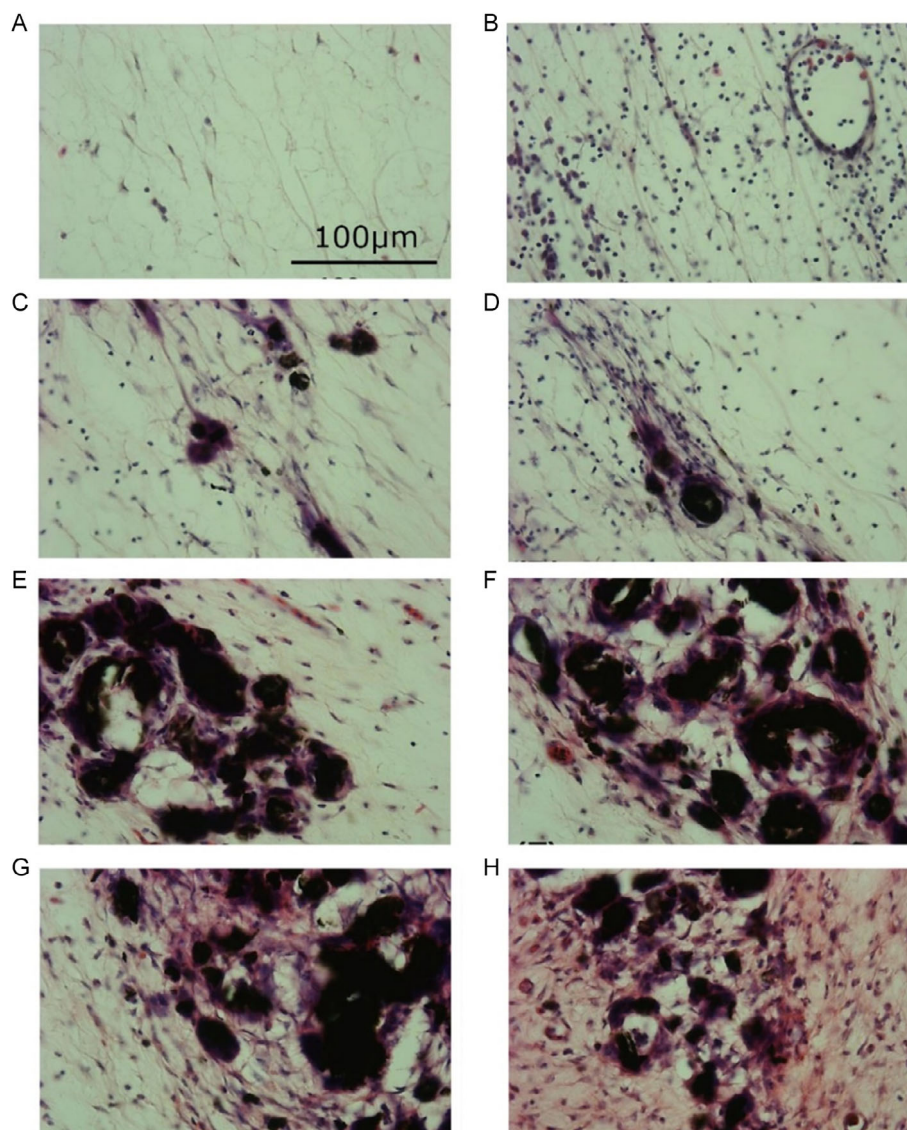
Figure 9. Microscope images of hematoxylin- and eosin-stained fixed growing feathers (GFs) injected with functionalized low oxygen graphene-based nanomaterial (GBN) or vehicle (phosphate-buffered saline [PBS]). Using 9-week-old, nonvaccinated, male light-brown Leghorn chickens, the dermis of 20 GFs per chicken was injected with 10 μL of either GBN (300 μg mL^{-1}) or vehicle (PBS). GFs were collected before, and 1, 3, 5, and 7 days postinjection. The objective of this study was to use the GFs of chickens as a minimally invasive cutaneous test site to assess and monitor leukocyte recruitment in response to intradermal GBN injection. Optical microscopy images of fixed tissue sections with hematoxylin and eosin stains prepared from growing feathers injected with either GBN (seen in black) or PBS vehicle. A) Before the injection; B) at 1 day postinjection, C–F) at 3 days postinjection, and G,H) at 5 days postinjection. GBN was shown as a black material within the tissue/cells. Adapted under the terms of the CC BY 4.0 licence.[120] Copyright 2017, The Authors. Published by John Wiley & Sons, Ltd.

of a human RBC showed no interference with the perception of hemoglobin. This indicates the possibility of studying the electrochemical behavior of hemoglobin directly from human blood.[30]

Moreover, graphene derivatives strengthened and enhanced the performance of existing solutions, such as glassy carbon. Even if the latter is preferred over other metals due to its high hydrogen overpotential, graphene-modified glassy carbon electrodes provide better selectivity in isomers with the same electroactive groups with overlapping redox signatures.[136] Each atom in a graphene or graphene-based sheet is a surface atom,

increasing the sensitivity of the electron transport and molecular interaction with adsorbed molecules. Therefore, electrodes coated with graphene or its derivatives can provide greater selectivity and increased sensitivity in directly detecting hemoglobin from RBCs and blood samples. This allows quantitative analysis of RBCs in blood samples for clinical malaria diagnosis. One can also consider using a metasurface or SPR with a ring or cross-shaped configuration based on graphene for early-stage malaria detection. SPRs are commonly used to detect and analyze ligand/cell or host/pathogen interactions, cell/cell contacts, and cellular reactions. These sensors operate based on a specific mechanism
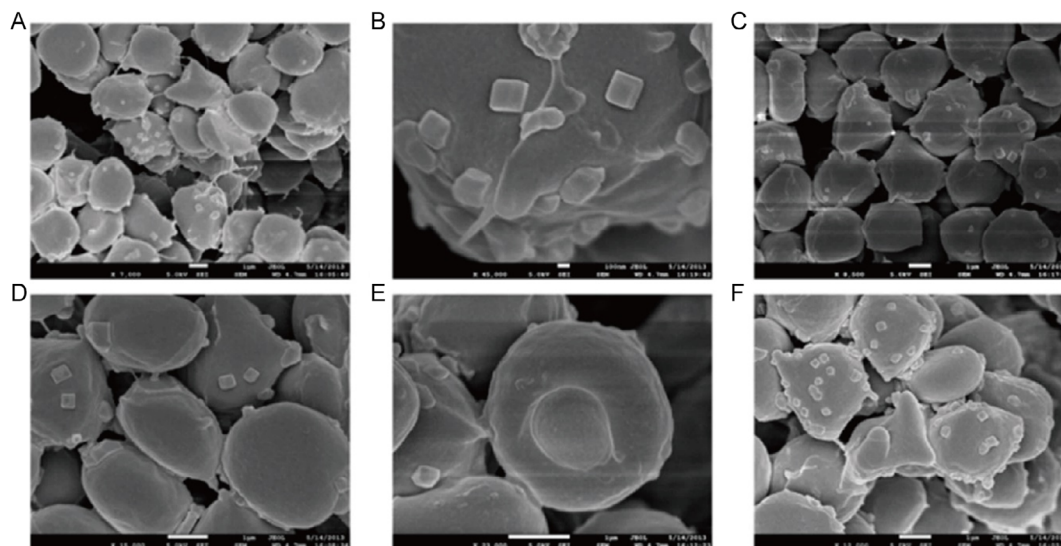
**ADVANCED
SCIENCE NEWS**

www.advancedsciencenews.com

**ADVANCED
NANOBIOMED
RESEARCH**
Open Access

www.advnanobiomedres.com

Figure 10. Scanning electron microscopy (SEM) images of RBCs before A–C) and after D–F) filtration at 5.0 kV with an average diameter of ≈3 μm. Upon confirming that the reduction signals observed in both lyophilized RBCs and lyophilized blood correspond to the reduction of hemoglobin, it becomes crucial to determine the source of these signals: 1) originating directly from RBCs or 2) arising from free hemoglobin released into the supernatant due to the lysis of RBCs. To address this, a lysis assessment was conducted. Notably, crystalline structures were identified on the membranes of the erythrocytes, suggesting their association with the sample preparation procedure. Adapted under the terms of the CC BY 4.0 licence.[30] Copyright 2014, The Authors. Published by Springer Nature.

that enables them to sense and measure minute changes in RI near a metal surface. As a result, SPRs are highly sensitive and can provide accurate and detailed information on the interactions of interest. Metasurfaces, artificially designed surfaces made up of subwavelength scatterers can enhance the sensitivity of graphene-based metasensors, or SPRs, by altering the interactions between light and matter. This modification can lead to improved performance and accuracy of the sensors. According to recent work, a graphene–metasurface sensor has been developed that can detect even minor variations with remarkable precision. This sensor has a maximum relative sensitivity of $300\,GHz\,RIU^{-1}$, while its figure of merit values range between 0.887 and $1.587\,RIU^{-1}$, making it highly effective in distinguishing between different transmittance dips.[137] A recent study presented the fabrication of a highly efficient biosensor utilizing a hybrid architecture of $SrTiO_3$ (STO) and graphene to detect malaria rapidly. The developed biosensor exhibits superior sensitivity, specificity, selectivity, and stability performance, making it a promising candidate for practical applications in disease diagnosis and biomedical research.[138] The SPR device being proposed combines a glass prism, silver (Ag), strontium titanate (STO), graphene, an affinity layer, and a sensing gel medium to enable the effective detection of schizont, trophozoite, and ring malaria stages.

The advances in field-effect transistors (FETs) and their integration as high-sensitivity biosensors[139–141] in the biomedical field have paved the way for graphene and its derivatives to be incorporated as channel material to replace the technologically limited silicon materials; in fact, aptamer-based FET (aptaFET) with silicon materials showed higher sensitivity and selectivity in detecting *Plasmodium falciparum* GDH (PfGDH) in blood, by measuring the changes in the gate potential in the FET

(**Figure 12**).[142] Replacing silicon material in the post-Moore's law era with a graphene-based semiconductor will further enhance these devices and provide more biosensing capabilities.[42] In an earlier study, Ang et al.[143] explored the use of graphene-based transistors for detecting RBCs infected with malaria. Their research highlighted the potential of using this technology for early and accurate malaria diagnosis in early stages. They showed a novel flow–catch–release-sensing mechanism of a single malaria-infected RBC on the graphene-based FET. The conductance changes with specific dwell times could differentiate the trophozoite and schizont forms of *P. falciparum*, the parasite erythrocytes, in two distinct structural manifestations. This study paved the way for fast future clinical diagnostic applications.

7. Prospects of TMDCs as Possible 2D Materials for Malaria Detection

As explained in the earlier sections, malaria is one of the most fatal vector-borne diseases affecting human health globally. The discussion of potential materials for malaria detection is mainly focused on graphene and its derivatives. The antimicrobial properties and biocompatibility of graphene and its derivatives make it a top choice for affordable health care diagnostics and promising biosensors.

The progress in biotechnology and nanotechnology has also yielded other innovative 2D materials, enabling the creation of cost-effective biosensor platforms with enhanced capabilities. With the recent advancements in graphene-based technologies, it is now possible for TMDCs to play a crucial role in the rapid diagnosis of malaria through their ability to provide ultrafast
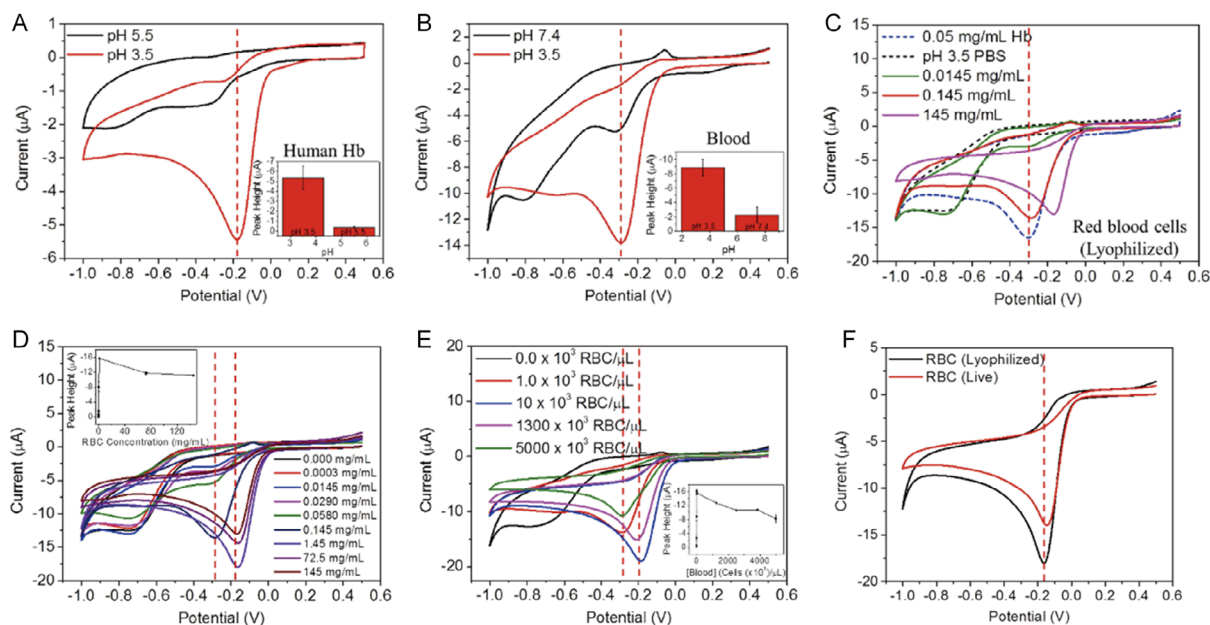
**ADVANCED
SCIENCE NEWS**

www.advancedsciencenews.com

**ADVANCED
NANOBIOMED
RESEARCH**

www.advnanobiomedres.com

Figure 11. Direct in vivo electrochemical detection of hemoglobin in red blood cells. The electrochemical behavior of iron ions in hemoglobin provides insight into the chemical activity in the red blood cell, which is important in the field of hematology. This study mainly contributed to detecting hemoglobin in human red blood cells on glassy carbon electrodes (GC). Cyclic voltammograms were acquired in aqueous 50 mM phosphate buffer at pH 3.5 to investigate the electrochemical reduction of A) human hemoglobin (0.05 mg mL^{-1}, 0.78 μM) at GC electrodes. The reduction peak potential of hemoglobin decreases with increasing pH. Inset: Reduction peak height of cyclic voltammograms at different pH values. B) Cyclic voltammograms were obtained in aqueous 50 mM phosphate buffer at pH 3.5 and pH 7.4 to study the electrochemical reduction of blood, with a blood concentration of 1×10^3 cells μL^{-1}. C) Cyclic voltammograms were acquired in aqueous 50 mM phosphate buffer at pH 3.5 to investigate the electrochemical reduction of RBCs (powder) at GC–Nf–RBC–3Nf electrodes. Control experiments were conducted using Hb (blue-dotted line) and pH 3.5 PBS (black-dotted line). D) Cyclic voltammograms were acquired in an aqueous 50 mM phosphate buffer at pH 3.5 to investigate the electrochemical reduction of RBCs at GC–Nf–RBC–3Nf electrodes. The legend shows the concentrations of RBC (mg mL^{-1}). Inset: Reduction peak height corresponding to different concentrations of RBC. The calibration curve exhibited concentration saturation starting at 1.45 mg mL^{-1} (50×10^3 cells μL^{-1}), with error bars representing RSD ($n = 3$; 95% confidence interval). E) Cyclic voltammograms were obtained in an aqueous 50 mM phosphate buffer at pH 3.5 to study the electrochemical reduction of blood at GC–Nf–B–3Nf electrodes. The legend shows the concentrations of blood (cells ($\times 10^3$) μL^{-1}). F) Cyclic voltammograms were acquired in aqueous 50 mM phosphate buffer at pH 3.5 to investigate the electrochemical reduction of RBCs (live) at GC–Nf–RBC–3Nf electrodes. A comparison was made between RBCs purchased from Sigma Aldrich in powder form (black line, RBCs suspended in pH 3.5 PBS, RBC concentration of 1.45 mg mL^{-1}, 50×10^3 cells μL^{-1}) and RBCs derived directly from blood samples (red line, RBCs suspended in pH 7.4 1 × PBS, RBC concentration of ≈10 vol%). The scan rate used was 0.1 V s^{-1}. Adapted under the terms of the CC BY 4.0 licence.[30] Copyright 2014, The Authors. Published by Springer Nature.

responses. The distinctive anisotropic structures, layered nature, and high surface areas of these materials make them ideal for creating various wearable or electrochemical sensors to detect malaria. So, importance must be given to TMDCs, which are not toxic and can be safely used in point-of-care diagnostics. It is worth noting that 2D hexagonal molybdenum sulfide, or 2H-MoS$_2$, is reported to have cytotoxicity levels even lower than those of graphene and similar layered materials.[144]

The synthesis of these 2D TMDCs is possible either as a top-down or bottom-up approach.[145] Most top-down methods involve the exfoliation of the commercial 2D TMDCs either mechanically using scotch tape or polydimethylsiloxane (PDMS) stamps (as reported for graphene exfoliation from graphite) or using fast-drying solvents like ethanol and isopropanol.[145] Yet the yield of the TMDCs is relatively low in such cases. So, bottom-up synthesis approaches can solve the scalability issues related to these materials.[145] More importantly, the crystallinity, phase, and microstructure of these 2D TMDCs can be manipulated via bottom-up synthesis approaches.[146]

Such synthesis routes focus on chemical vapor transport, CVD, molecular beam epitaxy, microwave irradiation, etc. Among the reported synthesis methods, CVD is excellent for addressing scalability and crystallinity concerns in producing TMDCs, making it the most preferred option among these available techniques. Usually, oxide- or metal-based precursors and elemental chalcogen sources are used to prepare TMDCs in the CVD.[146–149] A simple variation in reaction times, working pressures, amount of precursors used, working temperatures, etc., can create TMDCs with the desired material properties. Incorporating noble metal nanoparticles like gold (Au) and silver (Ag) onto TMDCs can enhance their optoelectronic properties and increase biocompatibility (such as by providing more precise signals using available surface plasmons in the 2D layers) without compromising their intrinsic qualities.

Multiple studies have revealed the significant binding abilities of layered TMDC nanosheets toward a diverse range of biomolecules.[150,151] Furthermore, the nanosheets can demonstrate exceptional fluorescence quenching capabilities, which can be
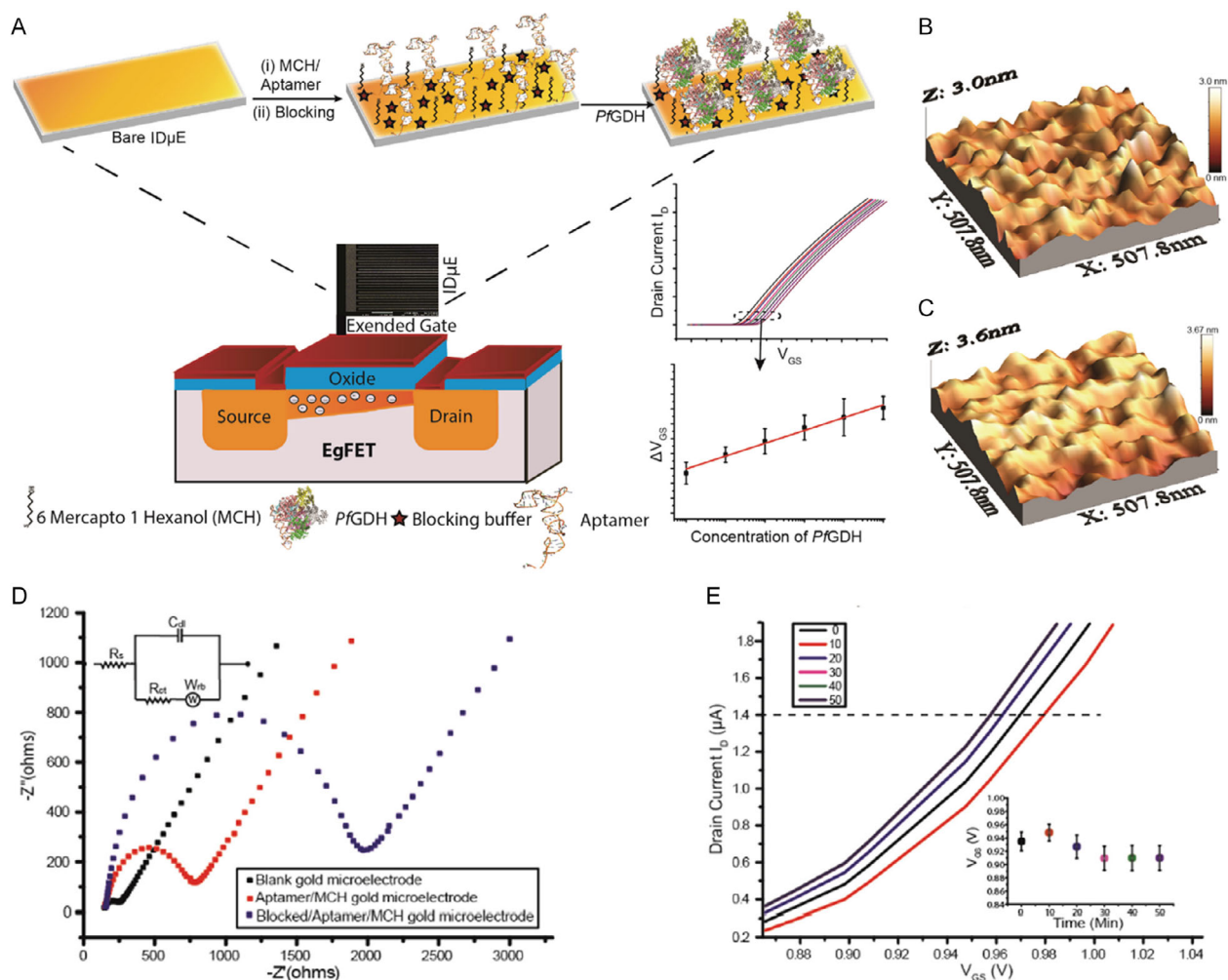
Figure 12. Fabrication process of aptamer-based field-effect transistor (aptaFET) for detecting the malaria biomarker PfGDH in blood and atomic force microscopy (AFM) characterization of IDµE. A) The detection uses an extended-gate field-effect transistor (FET) with a selective aptamer as the bio-recognition element targeting the PfGDH biomarker. The aptamer is immobilized on the interdigitated gold microelectrode (IDµE) connected to the gate of the transistor using gold–thiol chemistry. Atomic force microscopy is used to characterize B) the bare IDµE and C) the protein/aptamer–IDµE surfaces (scanned area ≈0.5 × 0.5 µm²). D) Electrochemical impedance spectroscopy characterization of blank and modified IDµEs. E) Stability studies of aptaFET in binding buffer, represented by the plot of drain current (I_D) versus gate voltage (V_{GS}) at different incubation times. The inset plot shows the gate voltage at a fixed drain current versus different incubation times. Adapted under the terms of the CC BY 4.0 licence.[142] Copyright 2018, The Authors. Published by Elsevier.

further exploited to create high-performance biomolecular sensing systems that offer excellent sensitivity and selectivity. It has been discovered that TMDC nanosheet aptasensors exhibit comparable or even superior detection limits compared to GO nanosheet aptasensors when detecting single-stranded DNA and protein targets, specifically thrombin and prostate-specific antigen.[152]

Among the many studied TMDCs, sulfide-based TMDCs (of the type MS₂) can be one of the possible materials to be used as fluorescence sensors in malaria detection. In this class of sensors, the sulfide-based TMDCs must show fluorescence emission while interacting with the aptamers. 2 H-MoS₂ possesses a suitable bandgap that enables it to exhibit photoluminescence in the visible range directly, unlike graphene, which usually lacks a

bandgap.[145] A recent study showcased a specialized aptamer for PLDH that was combined with 6-carboxyfluorescein (FAM) and a "capture release" fluorescent sensor based on single-layer MoS₂ nanosheets, allowing for the detection of PLDH[153] (**Figure 13** shows a detailed mechanism for early malaria detection using MoS₂ nanosheets). If the sample was negative for PLDH in the assay, the FAM-labeled aptamer was absorbed onto the surface of MoS₂ nanosheets through weak intermolecular forces, resulting in no fluorescence emission at 527 nm.[153] The fluorescence resonance energy transfer (FRET) process enables the MoS₂ nanosheets to receive fluorescence energy from FAM, as the aptamer and MoS₂ nanosheets were located within the Forster radius.[153] The aptamer, designed to target PLDH, detached from the MoS₂ nanosheet surface and formed a bond
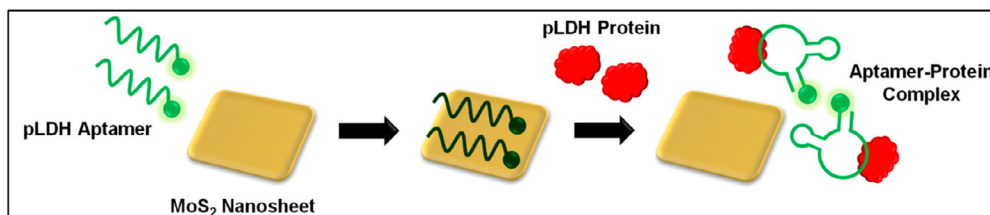
Figure 13. Illustration of aptamer-based "capture-release" assay for PLDH detection using MoS_2 nanosheets. Adapted under the terms of the CC BY 4.0 licence.[153] Copyright 2016, The Authors. Published by American Chemical Society Journals.

with the protein for positive samples. The FAM-labeled aptamer and MoS_2 nanosheets were positioned beyond the Forster radius, preventing FRET.

Consequently, the emission peak generated was directly proportional to the concentration of PLDH present in the sample.[153] Studies conducted on MoS_2 revealed its mode of action in FRET-based aptasensors, which manifests nonspecific fluorescence recovery.[154] The effectiveness of surface blocking in improving the sensors' specificity is also studied.[154] Su et al.[155] reported the dual-target electrochemical biosensing of AuNP-decorated MoS_2 nanosheets. For detecting adenosine triphosphate (ATP) and thrombin, researchers have utilized double-strand and hairpin aptamer probes with Mb and Fc labels.[155] This dual-target detection was based on AuNPs–MoS_2 nanocomposite structure.[155] Simultaneous immobilization of two aptamer probes was achieved on the electrode modified with AuNPs–MoS_2 film by forming an Au–S bond.[155] This advanced aptasensor shows high selectivity toward ultralow concentrations of thrombin and ATP as low as 0.0012 and 0.74 nM, respectively. Therefore, the aptasensor in this report is a viable option for detecting a variety of aptamers that bind to specific targets, as it is susceptible, facile, and cost-effective.[155] A highly selective paper-based MoS_2 nanosheet-mediated FRET aptasensor for rapid malaria diagnosis was reported by Geldert et al.[156] The researchers explored various paper types, encompassing laboratory-grade and everyday household products, as potential substrates for producing FRET-based aptasensors.[156]

In addition to MoS_2, tungsten disulfide or WS_2 can also be used as a potential 2D material to detect malaria. This is because optoelectronically sensitive TMDCs like WS_2 can be utilized to develop effective, biocompatible SPR sensors. In this case, possible ligand–target interactions can cause surface alterations and changes in RI on the chip, which these SPR sensors can potentially detect. Minute changes in the angle and intensity of reflected light can also occur due to variations in the RI caused by biological, physical, or chemical processes taking place on the surface of the chip. So, future works should utilize the enhanced SERS response of pristine WS_2 and noble-metal-functionalized WS_2 to develop more advanced point-of-care rapid diagnostics for early malaria detection.

Photonic crystals (PhCs) integrated into silicon-based photonic integrated circuits have shown great potential as a platform for lab-on-a-chip biosensing applications. PhC-based biosensors are characterized by a periodic structure with a spacing comparable to the wavelength of light, which induces significant changes in the RI. The periodic structure's photonic bandgap generates "defected modes" due to variations in RI, resulting

in a strong light–matter interaction region. PhC structures can come in different dimensions, including 1D, 2D, and 3D PhCs. The 1D platform is the simplest and consists of a periodic structure arranged in a planar format with layers of different materials. The manufacturing process for the 1D PhC structure is relatively straightforward compared to 2D or 3D structures. Although the sensitivity of a PhC biosensor is lower than that of the other optical biosensors, such as interferometers or resonators, it can be easily integrated onto a single chip with a high density volume and can detect multiple analytes. The inherent sensing property of this platform can be leveraged to detect malaria in its different stages with high efficiency.

PhC-based biosensors have become a popular choice for researchers in recent years. Chaudhary et al.[157] have engineered a susceptible PhC fiber (PCF)-based SPR biosensor designed to detect malaria disease at different stages. This plasmonic biosensor can be used to detect various blood compositions, including white blood cells, RBCs, hemoglobin, water, and plasma. The SPR–PCF-based dual-wavelength single-polarization filter presented by Chaudhary et al.[158] is a promising solution for detecting malaria with high precision and accuracy. Several other examples of biosensors based on plasmonic have been reported recently that employ D-shaped PCF SPR configuration with and without 2D materials such as graphene, MoS_2, and others. The sensitivity of these sensors has been significantly enhanced using 2D materials and variations in the geometry of PCF structures to improve bioanalyte adsorption and interaction between the core and plasmonic layer. For instance, a biosensor utilizing a PCF with a quasi-D-shaped configuration and an indium tin oxide–graphene combination achieves a sensitivity of $12\,000\ nm\ RIU^{-1}$ within the analyte range of 1.21–1.32 RI.[159] Another D-shaped PCF plasmonic sensor, designed for double peak detection, demonstrates a maximum sensitivity of $29\,000\ nm\ RIU^{-1}$, the RI range being 1.377–1.385 G.[160] A PCF-based SPR sensor with an open channel, which provides a sensitivity of $11\,500\ nm\ RIU^{-1}$,[161] has also been proposed. Notably, the use of 2D materials and variations in PCF geometry have also improved the resolution of these sensors. However, the manufacturing complexity of these sensors has also increased due to the use of such materials and structures. In their study, Srivastava et al.[162] demonstrated the successful use of a D-shaped PCF as a microchannel plasmon sensor. This was achieved through strong coupling between the deposited gold and the bioanalyte ligand, resulting in an effective sensing mechanism. Shafkat et al.[163] presented a single elliptical channel-based PCF sensor that utilizes a hexagonal arrangement of double loops of circular air holes. The sensor's design features

a horizontal elliptical channel located at the center of the fiber, which contains a sample of RBCs. The sensor's response was measured by observing the shift in the transmission spectra due to the changes in the RI of the RBCs during different stages of the parasite's life cycle.

8. Conclusion and Future Perspectives

Graphene and its 2D analogs have garnered significant attention within various disciplines, particularly in the biomedical field. Medical applications range from regenerative medicine to gene and drug delivery and cancer therapy.[164] However, the antimicrobial feature of graphene and its derivatives needs more research and investigation due to the reported aggregation and mode of exposure effect on graphene and related materials' cytotoxicity.[164] The oxygen content, dosage, surface functional groups, and structural defects are all parameters reported to affect this material's toxicity. The bioimpact of graphene-based materials is also a research topic that needs more data and relevant approaches, primarily through in vivo investigation.

In the fight against malaria, graphene and its 2D analog-based devices are commonly considered to cover both the preventive and the diagnosis phases. GO nanosheets cannot only physically obstruct the invasion of malaria parasites into RBCs effectively but also delay their progression from the ring to the trophozoite stage.[112]

In addition to the traditionally recognized role as a barrier to prevent mosquito bites, nanofabrication of GQDs with high toxicity against malaria mosquitoes and nano-DDS has been studied and proven valid. Interestingly, the predation efficiency of natural mosquito enemies (e.g., *Hoplobatrachus tigerinus*, *Anax immaculifrons*, and *Gambusia affinis*) was enhanced after post-treatment with GQDs.[108] A GQD-based antimalarial nano-DDS was verified effective on the cultured *P. falciparum* after 33 h of equilibrium release.[165]

In the fight against malaria, graphene-based devices can cover both the preventive and the diagnosis phases (as indicated in Table 1).[108,112,131,132,165–172] Most malaria diagnoses are based on RBC analysis of the subjects, but DNA detection using graphene-based materials is most promising.[173] DNA detection is considered an attractive application in disease diagnosis, including malaria, but there are two challenges facing this field:
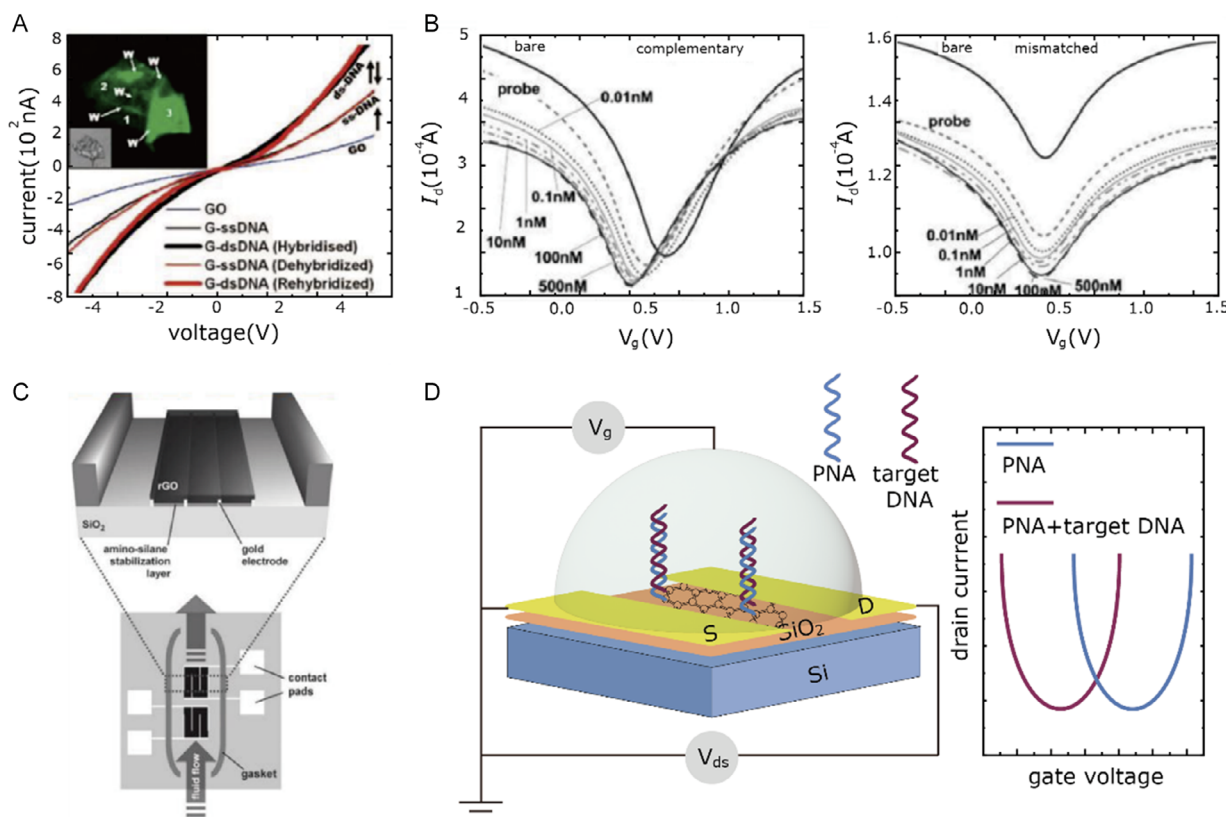

Figure 14. Graphene-based FET DNA detectors. A) DNA transistor: single-stranded DNA (ss-DNA) is tethered to graphene oxide (GO), resulting in increased conductivity of the device. Hybridization and dehybridization of DNA on the G-DNA device lead to reversible changes in conductivity. B) Transfer characteristics of graphene transistors: i) before adding DNA, ii) after immobilization with probe DNA, and iii) after reaction with complementary or one-base mismatched DNA molecules at concentrations ranging from 0.01 to 500 nM. C) Schematic representation of the sensor with a reference region; the enlarged area shows GO deposited on prefabricated electrodes. D) Schematic illustration of the rGO FET biosensor for DNA detection based on peptide nucleic acid (PNA)–DNA hybridization. The right part shows a typical current signal following PNA–DNA hybridization. Adapted under the terms of the CC BY 4.0 licence.[173] Copyright 2018, The Authors. Published by MDPI Journals.
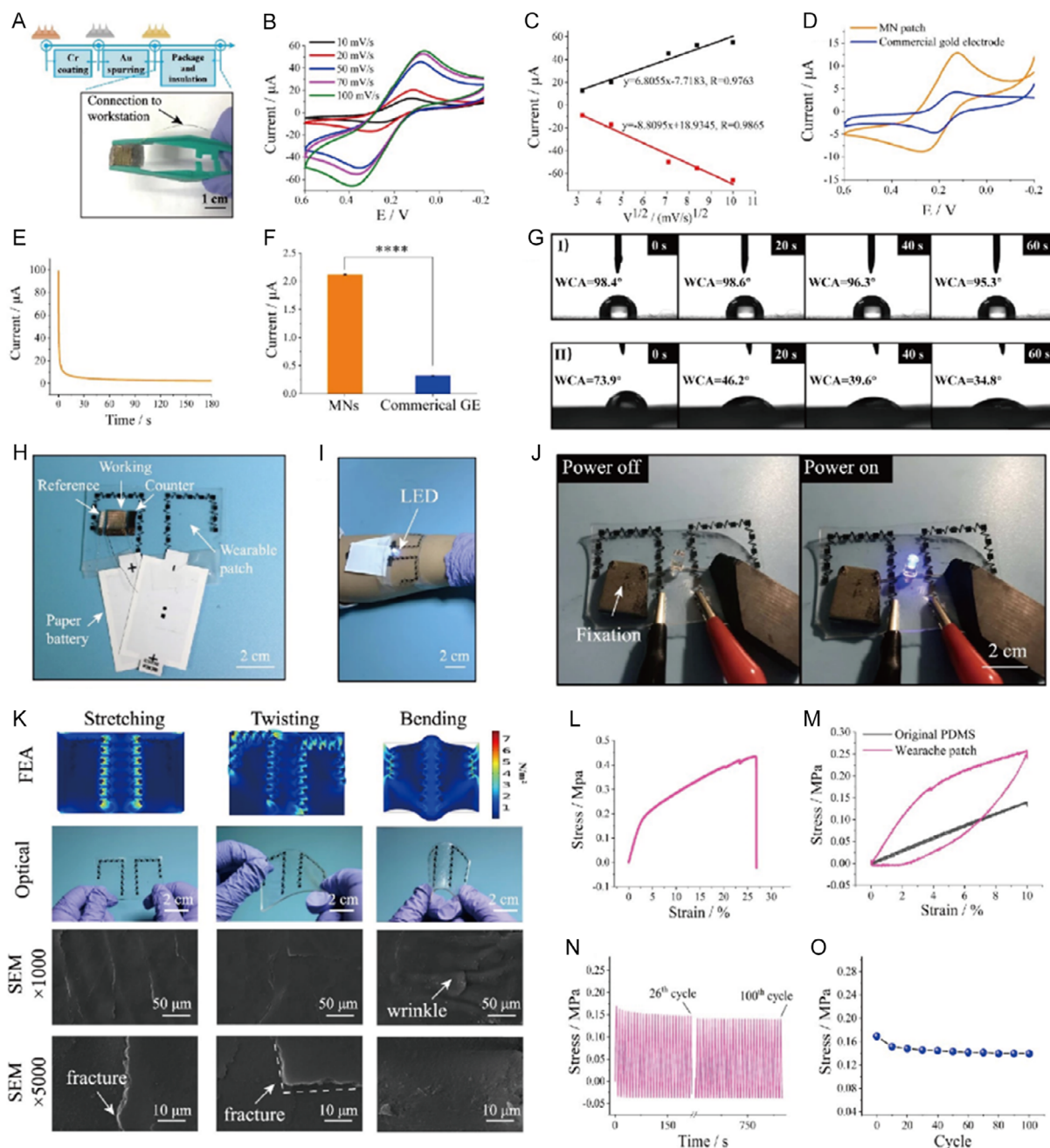
Figure 15. Fabrication, electrochemical, and mechanical properties of the graphene reinforced ionic liquid-cured styrene butadiene rubber (CRISPR) wearable patch. A) Schematic illustration of the conductive microneedles (MNs). B) Cyclic voltammetry (CV) plots of the as-fabricated conductive MNs at different scanning rates using a 1 mM $[Fe(CN)_6]^{3-}/^{4-}$ probe; quiet time: 2 s; sensitivity (A V^{-1}): 1×10^{-4} A V^{-1}. C) Relationship between the square root of the scanning rate and the corresponding peak current using a 1 mM $[Fe(CN)_6]^{3-}/^{4-}$ probe; quiet time: 2 s; sensitivity (A V^{-1}): 1×10^{-4} A V^{-1}. D) CV plots of the conductive MNs and commercial gold electrode using a 1 mM $[Fe(CN)_6]^{3-}/^{4-}$ probe; quiet time: 2 s; sensitivity (A V^{-1}): 1×10^{-4} A V^{-1}. E) Real-time current–time curve recorded by the conductive MNs in PBS buffer (0.01 M, pH 7.4); quiet time: 0 s; sensitivity (A V^{-1}): 1×10^{-3} A V^{-1}. F) Real-time current comparison between the conductive MNs and commercial gold electrode in PBS buffer (0.01 M, pH 7.4); $*p < 0.05$, $**p < 0.01$, $***p < 0.001$, $****p < 0.0001$, analyzed by two-way analysis of variance, p-value of 0.0000094, quiet time: 0 s; sensitivity (A V^{-1}): 1×10^{-3} A V^{-1}. G) Contact angle testing of water droplets on the surface of the I) original PDMS film and II) hydrophilic-treated PDMS film. H) Photograph of the CRISPR wearable patch based on reverse iontophoresis and three-electrode MNs. I) The printed wearable patch is mounted on the skin. J) A blue light-emitting diode powered by the wearable patch with a voltage of 6 V. K) Finite elemental analysis, optical photographs, and scanning electron microscopy (SEM) images of the wearable device under different mechanical distortions, including stretching, twisting, and bending; results obtained from three independent repeated experiments. L) Strain versus stress curve for the wearable patch. M) Single stretch–release cycle with 10% strain for two different membranes. N) Stress variation of the wearable patch in a 100-cycle test with a strain of 4%. O) Stress variation of the wearable patch. Adapted under the terms of the CC BY 4.0 licence.[185] Copyright 2022, The Authors. Published by Springer Nature Journals.

**ADVANCED
SCIENCE NEWS**

www.advancedsciencenews.com

**ADVANCED
NANOBIOMED
RESEARCH**

www.advnanobiomedres.com

the speed and the accuracy of the detection. The simple and less-expensive label-free DNA detection using graphene derivatives is an attractive attribute of the graphene properties, enabling it to be integrated into optical, electronic, and electrochemical biosensors. For instance, the integration of graphene in electronic biosensors can be made by using the DNA in the gating area, changing the transfer characteristics due to the n-doping phenomenon (**Figure 14**), and showing higher sensitivity compared to available biosensors.[174] Using recognition elements such as the DNA-mimicking PNA opens the way toward ultrafast detection.

The challenges toward appropriate DNA detection are related to the DNA translocation and the noise level encountered during the detection. The availability of different graphene derivatives with a wide range of properties and better control over modulations in the tunneling current within the graphene can solve these issues and provide high sensitivity and selectivity in DNA biosensors. In addition, rapid speed at DNA translocation leads to low signal-to-noise ratios and inaccuracies, as seen in sequence detection.[175] Graphene-based devices have been proposed as a potential solution to this challenge, as the ultrathin nature of graphene allows for precise control over the nanopore size and shape. Additionally, the high electrical conductivity of graphene enables real-time monitoring of the translocation process, which can help to reduce errors and improve sequencing accuracy.[176] Inheriting the flexibility of DNA molecules is another challenge in using nanopores for DNA sequencing, which can cause fluctuations in the translocation speed and make accurate sequencing more difficult.[175] This challenge is particularly relevant for longer DNA molecules, which are more likely to exhibit fluctuations and reduce sequencing accuracy. One approach to inhibiting DNA fluctuations in graphene-based nanopores is to modify the surface chemistry of the graphene to increase the interactions between the DNA and the graphene, leading to a tighter interaction between the DNA molecule and the graphene, reducing the likelihood of fluctuations during translocation.[177] Another approach is to use a hinged graphene membrane, which can move in response to the movement of the DNA molecule and reduce the fluctuations in translocation speed.[178]

Graphene-related nanomaterials are launching a new era in the fight against malaria; preventive measures can be enhanced using these materials in the new wearable technologies, providing more efficient and cheaper solutions. Diagnosis of malaria will also be enriched with compact and easy-to-deploy solutions such as electrochemical detection of hemoglobin and DNA detection devices based on graphene and its derivates. Moreover, it may be possible to provide a hybrid solution using a graphene device for direct parasite detection in the DNA and the oxidation states of the hemoglobin, of which high sensitivity and specificity of the test are desirable in the field settings.[12,179]

Graphene-related nanomaterials have become a fundamental material for the production of wearable sensors and contributed to a high level of mechanical robustness flexibility, optical transparency, and piezoresistive sensitivity[15,180,181] and engaged in research frequently[14,16,70,182,183] to advance the development of next-generation wearable electronic devices for applications in artificial intelligence, prosthetics, health care, and aerospace. Wearable sensors can be physically adhered to the human body or embedded in ready-to-wear textiles and other peripheral

products and are expected to play an essential role in health care, where vital signs are monitored. Graphene-related nanosheet-based sensors can output physiological information in electrical signals, that is, finger flexion, breathing, and heartbeat.[184] The integration of graphene into clothing and accessories has enabled the advancement of wearable devices with new functionalities, such as DNA detection and diagnosis.[185,186] An in-line wearable graphene-based microneedle patch for extraction and long-term in vivo monitoring of universal cell-free DNA was reported,[185] heralding the potential capacity for malaria detection (**Figure 15**).

Efforts toward malaria elimination will require collaboration and synergy among researchers and stakeholders. This is particularly important, as the world aims to eradicate the disease by 2050. The timely discovery and development of new materials and technologies, from preventive to diagnostic phases, is crucial. This review comprehensively discussed the latest breakthroughs in graphene-based technology, including wearable sensors, and their potential uses in combating malaria. We also address concerns regarding the compatibility and biosafety of graphene in the human body. MoS_2 and WS_2, related to 2D sulfide TMDC analogs of graphene, display considerable potential as emerging layered materials in aptamer and fluorescent sensors.

Moreover, the other sulfide-based 2D TMDCs that resemble graphene in structure possess multiple binding sites that can readily interact with single-stranded DNA/RNA through covalent, noncovalent, hydrogen bond, and π-stacking interactions. Such TMDC–aptamer-binding studies should be thoroughly pursued to understand the role of immunogenetics. A comprehensive understanding of 2D material-based sensors will unlock the potential to facilitate the rapid detection of malaria specimens in the human body. So, ex vivo, ultrafast responsive sensors can also be fabricated easily for malaria detection. Other than using pristine 2D TMDCs as possible sensors, noble metal functionalization of 2D materials will be of great interest, as they can help tune the optoelectronic properties. So, SPR-based 2D sensors can be engineered for prompt malaria detection. We believe our review article on graphene and its 2D analogs will inspire further research on their applications in combating malaria. We are confident that this article will usher in the development of new and innovative strategies to stop this deadly disease.

Acknowledgements

Conflict of Interest

The authors declare no conflict of interest.

Author Contributions

W.K.P., M.B., G.D.N., and A.E.M. designed the outline and the concept of the manuscript, and all authors analyzed the available data and did the

[1] World Malaria Report 2023, https://www.who.int/publications-detail-redirect/9789240086173 (accessed: January 2024).

[2] W. H. Organization, *From Malaria Control to Malaria Elimination: A Manual for Elimination Scenario Planning*, World Health Organization **2014**.

[3] R. G. A. Feachem, I. Chen, O. Akbari, A. Bertozzi-Villa, S. Bhatt, F. Binka, M. F. Boni, C. Buckee, J. Dieleman, A. Dondorp, A. Eapen, N. S. Feachem, S. Filler, P. Gething, R. Gosling, A. Haakenstad, K. Harvard, A. Hatefi, D. Jamison, K. E. Jones, C. Karema, R. N. Kamwi, A. Lal, E. Larson, M. Lees, N. F. Lobo, A. E. Micah, B. Moonen, G. Newby, X. Ning, et al., *Lancet* **2019**, *394*, 1056.

[4] W. K. Peng, T. F. Kong, C. S. Ng, L. Chen, Y. Huang, A. A. S. Bhagat, N.-T. Nguyen, P. R. Preiser, J. Han, *Nat. Med.* **2014**, *20*, 1069.

[5] T. Fook Kong, W. Ye, W. K. Peng, H. Wei Hou, . Marcos, P. R. Preiser, N.-T. Nguyen, J. Han, *Sci. Rep.* **2015**, *5*, 11425.

[6] A. Dupré, K.-M. Lei, P.-I. Mak, R. P. Martins, W. K. Peng, *Microelectron. Eng.* **2019**, *209*, 66.

[7] F. D. Krampa, Y. Aniweh, P. Kanyong, G. A. Awandare, *Sensors* **2020**, *20*, 799.

[8] S. Aggarwal, W. K. Peng, S. Srivastava, *Diagnostics* **2021**, *11*, 2222.

[9] A. D. T. Costa, A. C. C. Aguiar, A. M. Silva, D. B. Pereira, A. D. T. Costa, A. C. C. Aguiar, A. M. Silva, D. B. Pereira, *IntechOpen* **2021**, https://doi.org/10.5772/intechopen.96721.

[10] W. Wang, Z. Zheng, C. Yang, Z. Fang, S. Wang, C. Yuen, K. Tang, Q. Liu, P. Preiser, Y. Zheng, *IEEE Trans. Instrum. Meas.* **2022**, *71*, 1.

[11] J. Han, W. K. Peng, *Nat. Med.* **2015**, *21*, 1387.

[12] M. I. Veiga, W. K. Peng, *Malar. J.* **2020**, *19*, 68.

[13] M. Pelin, H. Lin, A. Gazzi, S. Sosa, C. Ponti, A. Ortega, A. Zurutuza, E. Vázquez, M. Prato, A. Tubaro, A. Bianco, *Nanomaterials* **2020**, *10*, 1602.

[14] Y. Qiao, Y. Wang, H. Tian, M. Li, J. Jian, Y. Wei, Y. Tian, D.-Y. Wang, Y. Pang, X. Geng, X. Wang, Y. Zhao, H. Wang, N. Deng, M. Jian, Y. Zhang, R. Liang, Y. Yang, T.-L. Ren, *ACS Nano* **2018**, *12*, 8839.

[15] E. Singh, M. Meyyappan, H. S. Nalwa, *ACS Appl. Mater. Interfaces* **2017**, *9*, 34544.

[16] D. Kireev, S. K. Ameri, A. Nederveld, J. Kampfe, H. Jang, N. Lu, D. Fabrication Akinwande, *Nat. Protoc.* **2021**, *16*, 2395.

[17] Y. Qiao, X. Li, T. Hirtz, G. Deng, Y. Wei, M. Li, S. Ji, Q. Wu, J. Jian, F. Wu, *Nanoscale* **2019**, *11*, 18923.

[18] A. Mbanefo, N. Kumar, *Trop. Med. Infect. Dis.* **2020**, *5*, 102.

[19] V. Baptista, W. K. Peng, G. Minas, M. I. Veiga, S. O. Catarino, *Biosensors* **2022**, *12*, 110.

[20] A. D. T. Costa, J. F. L. Santos, *Front. Cell. Infect. Microbiol.* **2022**, *12*, 1755.

[21] P. K. Sarswat, M. L. Free, *J. Electrochem. Soc.* **2019**, *166*, B1.

[22] A. Kumar, P. Verma, P. Jindal, *Optik* **2023**, *274*, 170549.

[23] S. Roy, S. Mondal, K. Debnath, *IEEE Sens. J.* **2023**, *23*, 285.

[24] S. Peng, Q. Wang, G. Xiong, S. C. B. Gopinath, G. Lei, *Biotechnol. Appl. Biochem.* **2022**, *69*, 1354.

[25] N. Chauhan, T. Maekawa, D. N. S. Kumar, *J. Mater. Res.* **2017**, *32*, 2860.

[26] L. N. Borgheti-Cardoso, M. S. Anselmo, E. Lantero, A. Lancelot, J. L. Serrano, S. Hernández-Ainsa, X. Fernàndez-Busquets, T. Sierra, *J. Mater. Chem. B* **2020**, *8*, 9428.

[27] I. Irkham, A. U. Ibrahim, P. C. Pwavodi, F. Al-Turjman, Y. W. Hartati, *Sensors* **2023**, *23*, 2240.

[28] P. Zamzam, P. Rezaei, Y. I. Abdulkarim, O. Mohsen Daraei, *Opt. Laser Technol.* **2023**, *163*, 109444.

[29] K. Kenry, Y. B. Lim, M. H. Nai, J. Cao, K. P. Loh, C. T. Lim, *Nanoscale* **2017**, *9*, 14065.

[30] R. J. Toh, W. K. Peng, J. Han, M. Pumera, *Sci. Rep.* **2014**, *4*, 6209.

[31] R. J. Toh, W. K. Peng, J. Han, M. Pumera, *RSC Adv.* **2014**, *4*, 8050.

[32] A. K. Geim, K. S. Novoselov, *Nat. Mater.* **2007**, *6*, 183.

[33] A. K. Geim, *Science* **2009**, *324*, 1530.

[34] K. S. Novoselov, A. K. Geim, S. V. Morozov, D. Jiang, Y. Zhang, S. V. Dubonos, I. V. Grigorieva, A. A. Firsov, *Science* **2004**, *306*, 666.

[35] Y. Z. N. Htwe, M. Mariatti, *J. Sci.: Adv. Mater. Devices* **2022**, *7*, 100435.

[36] M. Y. Morozov, V. V. Popov, M. Ryzhii, V. G. Leiman, V. Mitin, M. S. Shur, T. Otsuji, V. Ryzhii, V. Ryzhii, V. Ryzhii, *Opt. Mater. Express* **2019**, *9*, 4061.

[37] B. Fadeel, C. Bussy, S. Merino, E. Vázquez, E. Flahaut, F. Mouchet, L. Evariste, L. Gauthier, A. J. Koivisto, U. Vogel, C. Martín, L. G. Delogu, T. Buerki-Thurnherr, P. Wick, D. Beloin-Saint-Pierre, R. Hischier, M. Pelin, F. Candotto Carniel, M. Tretiach, F. Cesca, F. Benfenati, L. Scaini, L. Ballerini, K. Kostarelos, M. Prato, A. Bianco, *ACS Nano* **2018**, *12*, 10582.

[38] J. A. Delgado-Notario, V. Clericò, E. Diez, J. E. Velázquez-Pérez, T. Taniguchi, K. Watanabe, T. Otsuji, Y. M. Meziani, *APL Photonics* **2020**, *5*, 066102.

[39] M. Sang, J. Shin, K. Kim, K. J. Yu, *Nanomaterials* **2019**, *9*, 374.

[40] V. Ryzhii, V. Ryzhii, V. Ryzhii, M. Ryzhii, V. Mitin, M. S. Shur, T. Otsuji, *Opt. Express* **2020**, *28*, 2480.

[41] V. Mitin, V. Ryzhii, T. Otsuji, V. Ryzhii, T. Otsuji, *Graphene-Based Terahertz Electronics and Plasmonics: Detector and Emitter Concepts*, Jenny Stanford Publishing **2020**, https://doi.org/10.1201/9780429328398.

[42] [2006.11881] Review: Graphene-based biosensor for Viral Detection, https://arxiv.org/abs/2006.11881 (accessed: July 2020).

[43] A. Hijazi, A. E. Moutaouakil, in *2019 44th Int. Conf. Infrared, Millimeter, and Terahertz Waves (IRMMW-THz)*, IEEE, Paris, France **2019**, pp. 1–2, https://doi.org/10.1109/IRMMW-THz.2019.8873712.

[44] A. E. Moutaouakil, H.-C. Kang, H. Handa, H. Fukidome, T. Suemitsu, E. Sano, M. Suemitsu, T. Otsuji, *Jpn. J. Appl. Phys.* **2011**, *50*, 070113.

[45] Y. M. Meziani, E. Garcia, E. Velazquez, E. Diez, A. El Moutaouakil, T. Otsuji, K. Fobelets, *Semicond. Sci. Technol.* **2011**, *26*, 105006.

[46] A. E. Moutaouakil, T. Watanabe, C. Haibo, T. Komori, T. Nishimura, T. Suemitsu, T. Otsuji, *J. Phys.: Conf. Ser.* **2009**, *193*, 012068.

[47] A. E. Moutaouakil, T. Suemitsu, T. Otsuji, D. Coquillat, W. Knap, in *35th Int. Conf. Infrared, Millimeter, and Terahertz Waves*, IEEE, Rome, Italy **2010**, pp. 1–2, https://doi.org/10.1109/ICIMW.2010.5612598.

[48] A. E. Moutaouakil, T. Komori, K. Horiike, T. Suemitsu, T. Otsuji, *IEICE Trans. Electron.* **2010**, *E93.C*, 1286.

[49] A. El Moutaouakil, T. Suemitsu, T. Otsuji, H. Videlier, S.-A. Boubanga-Tombet, D. Coquillat, W. Knap, *Phys. Status Solidi C* **2011**, *8*, 346.

[50] A. E. Moutaouakil, T. Suemitsu, T. Otsuji, D. Coquillat, W. Knap, *J. Nanosci. Nanotechnol.* **2012**, *12*, 6737.

[51] K. S. Novoselov, D. Jiang, F. Schedin, T. J. Booth, V. V. Khotkevich, S. V. Morozov, A. K. Geim, *Proc. Natl. Acad. Sci.* **2005**, *102*, 10451.

[52] K. A. Ritter, J. W. Lyding, *Nat. Mater.* **2009**, *8*, 235.

[53] C. N. R. Rao, K. Biswas, K. S. Subrahmanyam, A. Govindaraj, *J. Mater. Chem.* **2009**, *19*, 2457.

[54] P. Avouris, C. Dimitrakopoulos, *Mater. Today* **2012**, *15*, 86.

[55] Y. Zhang, Y.-W. Tan, H. L. Stormer, P. Kim, *Nature* **2005**, *438*, 201.

[56] X. Du, I. Skachko, A. Barker, E. Y. Andrei, *Nat. Nanotechnol.* **2008**, *3*, 491.

[57] A. H. Castro Neto, F. Guinea, N. M. R. Peres, K. S. Novoselov, A. K. Geim, *Rev. Mod. Phys.* **2009**, *81*, 109.

[58] R. R. Nair, H. A. Wu, P. N. Jayaram, I. V. Grigorieva, A. K. Geim, *Science* **2012**, *335*, 442.

[59] C. J. Castilho, D. Li, M. Liu, Y. Liu, H. Gao, R. H. Hurt, *Proc. Natl. Acad. Sci.* **2019**, *116*, 18304.

[60] D. Paret, P. Crego, P. Solere, *Smart Patches: Biosensors, Graphene, and Intra-Body Communications*, John Wiley & Sons **2023**.

[61] K. K. Sonigara, J. V. Vaghasiya, C. C. Mayorga-Martinez, M. Pumera, *Chem. Eng. J.* **2023**, *473*, 145204.

[62] J. Sengupta, C. M. Hussain, *TrAC Trends Anal. Chem.* **2023**, 117254.

[63] C. Coelho, G. Machado Jr., *Adv. Mater. Interfaces* **2022**, *9*, 2200177.

[64] L. Feng, L. Wu, X. Qu, *Adv. Mater.* **2013**, *25*, 168.

[65] E. Morales-Narváez, A. Merkoçi, *Adv. Mater.* **2012**, *24*, 3298.

[66] R. R. Nair, W. Ren, R. Jalil, I. Riaz, V. G. Kravets, L. Britnell, P. Blake, F. Schedin, A. S. Mayorov, S. Yuan, M. I. Katsnelson, H.-M. Cheng, W. Strupinski, L. G. Bulusheva, A. V. Okotrub, I. V. Grigorieva, A. N. Grigorenko, K. S. Novoselov, A. K. Geim, *Small* **2010**, *6*, 2877.

[67] J. Yao, Y. Sun, M. Yang, Y. Duan, *J. Mater. Chem.* **2012**, *22*, 14313.

[68] L. M. Bellan, D. Wu, R. S. Langer, *Wiley Interdiscip. Rev. Nanomed. Nanobiotechnol.* **2011**, *3*, 229.

[69] P. Suvarnaphaet, S. Pechprasarn, *Sensors* **2017**, *17*, 2161.

[70] Z. Li, Z. Yao, A. A. Haidry, Y. Luan, Y. Chen, B. Y. Zhang, K. Xu, R. Deng, N. Duc Hoa, J. Zhou, J. Z. Ou, *Nano Today* **2021**, *40*, 101287.

[71] M. Telkhozhayeva, E. Teblum, R. Konar, O. Girshevitz, I. Perelshtein, H. Aviv, Y. R. Tischler, G. D. Nessim, *Langmuir* **2021**, *37*, 4504.

[72] Y. Huang, E. Sutter, N. N. Shi, J. Zheng, T. Yang, D. Englund, H.-J. Gao, P. Sutter, *ACS Nano* **2015**, *9*, 10612.

[73] P. Yu, S. E. Lowe, G. P. Simon, Y. L. Zhong, *Curr. Opin. Colloid Interface Sci.* **2015**, *20*, 329.

[74] A. E. D. R. Castillo, V. Pellegrini, A. Ansaldo, F. Ricciardella, H. Sun, L. Marasco, J. Buha, Z. Dang, L. Gagliani, E. Lago, N. Curreli, S. Gentiluomo, F. Palazon, M. Prato, R. Oropesa-Nuñez, P. S. Toth, E. Mantero, M. Crugliano, A. Gamucci, A. Tomadin, M. Polini, F. Bonaccorso, *Mater. Horiz.* **2018**, *5*, 890.

[75] B. Gupta, M. Notarianni, N. Mishra, M. Shafiei, F. Iacopi, N. Motta, *Carbon* **2014**, *68*, 563.

[76] I. A. Kostogrud, E. V. Boyko, D. V. Smovzh, *Mater. Today: Proc.* **2017**, *4*, 11476.

[77] L. Sun, B. Chen, W. Wang, Y. Li, X. Zeng, H. Liu, Y. Liang, Z. Zhao, A. Cai, R. Zhang, Y. Zhu, Y. Wang, Y. Song, Q. Ding, X. Gao, H. Peng, Z. Li, L. Lin, Z. Liu, *ACS Nano* **2022**, *16*, 285.

[78] M. Lebioda, R. Pawlak, W. Szymański, W. Kaczorowski, A. Jeziorna, *Sensors* **2020**, *20*, 2134.

[79] S. Kumar, S. Gonen, A. Friedman, L. Elbaz, G. D. Nessim, *Carbon* **2017**, *120*, 419.

[80] A. T. Smith, A. M. LaChance, S. Zeng, B. Liu, L. Sun, *Nano Mater. Sci.* **2019**, *1*, 31.

[81] G. Machado, M. F. Cerqueira, J. Borme, M. Martins, J. Gaspar, P. Alpuim, *Mater. Chem. Phys.* **2020**, *256*, 123665.

[82] Y. Zhu, S. Murali, W. Cai, X. Li, J. W. Suk, J. R. Potts, R. S. Ruoff, *Adv. Mater.* **2010**, *22*, 3906.

[83] M. Pumera, *Chem. Rec.* **2009**, *9*, 211.

[84] O. Marciano, S. Gonen, N. Levy, E. Teblum, R. Yemini, G. D. Nessim, S. Ruthstein, L. Elbaz, *Langmuir* **2016**, *32*, 11672.

[85] C. A. Ferrari, F. Bonaccorso, V. Fal'ko, S. K. Novoselov, S. Roche, P. Bøggild, S. Borini, L. Koppens, V. Palermo, N. Pugno, J. A. Garrido, R. Sordan, A. Bianco, L. Ballerini, M. Prato, E. Lidorikis, J. Kivioja, C. Marinelli, T. Ryhänen, A. Morpurgo, N. J. Coleman, V. Nicolosi, L. Colombo, A. Fert, M. Garcia-Hernandez, A. Bachtold, F. G. Schneider, F. Guinea, C. Dekker, M. Barbone, et al., *Nanoscale* **2015**, *7*, 4598.

[86] K. Yang, Y. Li, X. Tan, R. Peng, Z. Liu, *Small* **2013**, *9*, 1492.

[87] A. Bianco, *Angew. Chem., Int. Ed.* **2013**, *52*, 4986.

[88] L. Ou, B. Song, H. Liang, J. Liu, X. Feng, B. Deng, T. Sun, L. Shao, *Part. Fibre Toxicol.* **2016**, *13*, 57.

[89] K. Wang, J. Ruan, H. Song, J. Zhang, Y. Wo, S. Guo, D. Cui, *Nanoscale Res. Lett.* **2010**, *6*, 8.

[90] A. Schinwald, F. A. Murphy, A. Jones, W. MacNee, K. Donaldson, *ACS Nano* **2012**, *6*, 736.

[91] X. Guo, N. Mei, *J. Food Drug Anal.* **2014**, *22*, 105.

[92] M. Xu, J. Zhu, F. Wang, Y. Xiong, Y. Wu, Q. Wang, J. Weng, Z. Zhang, W. Chen, S. Liu, *ACS Nano* **2016**, *10*, 3267.

[93] N. R. Jacobsen, G. Pojana, P. White, P. Møller, C. A. Cohn, K. Smith Korsholm, U. Vogel, A. Marcomini, S. Loft, H. Wallin, *Environ. Mol. Mutagen.* **2008**, *49*, 476.

[94] S. Bengtson, K. Kling, A. M. Madsen, A. W. Noergaard, N. R. Jacobsen, P. A. Clausen, B. Alonso, A. Pesquera, A. Zurutuza, R. Ramos, H. Okuno, J. Dijon, H. Wallin, U. Vogel, *Environ. Mol. Mutagen.* **2016**, *57*, 469.

[95] K. Yang, J. Wan, S. Zhang, B. Tian, Y. Zhang, Z. Liu, *Biomaterials* **2012**, *33*, 2206.

[96] N. Morimoto, T. Kubo, Y. Nishina, *Sci. Rep.* **2016**, *6*, 21715.

[97] W. Hu, C. Peng, M. Lv, X. Li, Y. Zhang, N. Chen, C. Fan, Q. Huang, *ACS Nano* **2011**, *5*, 3693.

[98] S. Liu, T. H. Zeng, M. Hofmann, E. Burcombe, J. Wei, R. Jiang, J. Kong, Y. Chen, *ACS Nano* **2011**, *5*, 6971.

[99] T. Devasena, A. P. Francis, S. Ramaprabhu, in *Reviews of Environmental Contamination and Toxicology*, Vol. 259 (Ed: P. de Voogt), Springer International Publishing, Cham **2021**, pp. 51–76, https://doi.org/10.1007/398_2021_78.

[100] M. Kryuchkova, R. Fakhrullin, *Environ. Sci. Technol. Lett.* **2018**, *5*, 295.

[101] Y. Li, L. Feng, X. Shi, X. Wang, Y. Yang, K. Yang, T. Liu, G. Yang, Z. Liu, *Small* **2014**, *10*, 1544.

[102] W. Majeed, S. Bourdo, D. M. Petibone, V. Saini, K. B. Vang, Z. A. Nima, K. M. Alghazali, E. Darrigues, A. Ghosh, F. Watanabe, *J. Appl. Toxicol.* **2017**, *37*, 462.

[103] A. M. Jastrzębska, P. Kurtycz, A. R. Olszyna, *J. Nanopart. Res.* **2012**, *14*, 1.

[104] F. van Breugel, J. Riffell, A. Fairhall, M. H. Dickinson, *Curr. Biol.* **2015**, *25*, 2123.

[105] M. Kelly, C.-Y. Su, C. Schaber, J. R. Crowley, F.-F. Hsu, J. R. Carlson, A. R. Odom, *MBio* **2015**, *6*, e00235.

[106] W. H. Organization, *World Malaria Report 2022*, World Health Organization **2022**.

[107] R. N'Guessan, V. Corbel, M. Akogbéto, M. Rowland, *Emerging Infect. Dis.* **2007**, *13*, 199.

[108] K. Murugan, D. Nataraj, A. Jaganathan, D. Dinesh, S. Jayashanthini, C. M. Samidoss, M. Paulpandi, C. Panneerselvam, J. Subramaniam, A. T. Aziz, M. Nicoletti, S. Kumar, A. Higuchi, G. Benelli, *J. Cluster Sci.* **2017**, *28*, 393.

[109] A. B. Seabra, A. J. Paula, R. de Lima, O. L. Alves, N. Durán, *Chem. Res. Toxicol.* **2014**, *27*, 159.

[110] M. C. Duch, G. R. S. Budinger, Y. T. Liang, S. Soberanes, D. Urich, S. E. Chiarella, L. A. Campochiaro, A. Gonzalez, N. S. Chandel, M. C. Hersam, G. M. Mutlu, *Nano Lett.* **2011**, *11*, 5201.

[111] B. Manjunatha, E. Seo, S. H. Park, R. R. Kundapur, S. J. Lee, *Environ. Sci. Pollut. Res.* **2021**, *28*, 34664.

[112] . Kenry, Y. B. Lim, M. H. Nai, J. Cao, K. P. Loh, C. T. Lim, *Nanoscale* **2017**, *9*, 14065.

[113] N. Malhotra, O. B. Villaflores, G. Audira, P. Siregar, J.-S. Lee, T.-R. Ger, C.-D. Hsiao, *Molecules* **2020**, *25*, 3618.

[114] H. N. Nguyen, C. Chaves-Lopez, R. C. Oliveira, A. Paparella, D. F. Rodrigues, *Carbon* **2019**, *143*, 419.

[115] D. Zhang, Z. Zhang, Y. Liu, M. Chu, C. Yang, W. Li, Y. Shao, Y. Yue, R. Xu, *Biomaterials* **2015**, *68*, 100.

[116] Biodistribution and Pulmonary Toxicity of Intratracheally Instilled Graphene Oxide in Mice | NPG Asia Materials, https://www.nature.com/articles/am20137 (accessed: May 2023).

[117] A. Shvedova, V. Castranova, E. Kisin, D. Schwegler-Berry, A. Murray, V. Gandelsman, A. Maynard, P. Baron, *J. Toxicol. Environ. Health, Part A* **2003**, *66*, 1909.

[118] K.-H. Liao, Y.-S. Lin, C. W. Macosko, C. L. Haynes, *ACS Appl. Mater. Interfaces* **2011**, *3*, 2607.

[119] M. Pelin, L. Fusco, V. León, C. Martín, A. Criado, S. Sosa, E. Vázquez, A. Tubaro, M. Prato, *Sci. Rep.* **2017**, *7*, 40572.

[120] G. F. Erf, D. M. Falcon, K. S. Sullivan, S. E. Bourdo, *J. Appl. Toxicol.* **2017**, *37*, 1317.

[121] R. Li, L. M. Guiney, C. H. Chang, N. D. Mansukhani, Z. Ji, X. Wang, Y.-P. Liao, W. Jiang, B. Sun, M. C. Hersam, A. E. Nel, T. Xia, *ACS Nano* **2018**, *12*, 1390.

[122] T. Lammel, P. Boisseaux, M.-L. Fernández-Cruz, J. M. Navas, *Part. Fibre Toxicol.* **2013**, *10*, 27.

[123] N. Rahmanian, M. Eskandani, J. Barar, Y. Omidi, *J. Drug Targeting* **2017**, *25*, 202.

[124] H. Kim, S. Lee, *Text. Res. J.* **2019**, *89*, 4114.

[125] V. C. Sanchez, A. Jachak, R. H. Hurt, A. B. Kane, *Chem. Res. Toxicol.* **2012**, *25*, 15.

[126] H. Itoh, M. Nishino, H. Hatabu, *J. Thorac. Imaging* **2004**, *19*, 221.

[127] J. Zhao, B. Deng, M. Lv, J. Li, Y. Zhang, H. Jiang, C. Peng, J. Li, J. Shi, Q. Huang, *Adv. Healthcare Mater.* **2013**, *2*, 1259.

[128] W.-P. Xu, L.-C. Zhang, J.-P. Li, Y. Lu, H.-H. Li, Y.-N. Ma, W.-D. Wang, S.-H. Yu, *J. Mater. Chem.* **2011**, *21*, 4593.

[129] World Health Organization, *World Malaria Report 2019*, Rorld Health Organization: S.l. **2019**.

[130] G. Dutta, *Mater. Sci. Energy Technol.* **2020**, *3*, 150.

[131] F. Wu, J. Singh, P. A. Thomas, Q. Ge, V. G. Kravets, P. J. Day, A. N. Grigorenko, *2D Mater.* **2020**, *7*, 045019.

[132] A. Uniyal, B. Chauhan, A. Pal (Preprint), In Review **2022**, https://doi.org/10.21203/rs.3.rs-1766754/v1.

[133] W. K. Peng, L. Chen, J. Han, *Rev. Sci. Instrum.* **2012**, *83*, 095115.

[134] W. K. Peng, A. Samoson, M. Kitagawa, *Chem. Phys. Lett.* **2008**, *460*, 531.

[135] P. Jain, B. Chakma, S. Patra, P. Goswami, *BioMed Res. Int.* **2014**, https://doi.org/10.1155/2014/852645.

[136] L. Chen, Y. Tang, K. Wang, C. Liu, S. Luo, *Electrochem. Commun.* **2011**, *13*, 133.

[137] J. Wekalao, S. K. Patel, N. K. Anushkannan, O. Alsalman, J. Surve, J. Parmar, *Diamond Relat. Mater.* **2023**, *139*, 110401.

[138] A. H. M. Almawgani, S. A. Taya, M. A. Abutailkh, K. M. Abohassan, A. T. Hindi, I. Colak, A. Pal, S. K. Patel, *Mod. Phys. Lett. B* **2023**, *37*, 2350190.

[139] N. Formisano, N. Bhalla, M. Heeran, J. Reyes Martinez, A. Sarkar, M. Laabei, P. Jolly, C. R. Bowen, J. T. Taylor, S. Flitsch, P. Estrela, *Biosens. Bioelectron.* **2016**, *85*, 103.

[140] T. S. Pui, P. Kongsuphol, S. K. Arya, T. Bansal, *Sens. Actuators, B* **2013**, *181*, 494.

[141] S. Cheng, S. Hideshima, S. Kuroiwa, T. Nakanishi, T. Osaka, *Sens. Actuators, B* **2015**, *212*, 329.

[142] N. K. Singh, P. D. Thungon, P. Estrela, P. Goswami, *Biosens. Bioelectron.* **2019**, *123*, 30.

[143] P. K. Ang, A. Li, M. Jaiswal, Y. Wang, H. W. Hou, J. T. L. Thong, C. T. Lim, K. P. Loh, *Nano Lett.* **2011**, *11*, 5240.

[144] W. Z. Teo, E. L. K. Chng, Z. Sofer, M. Pumera, *Chem. - Eur. J.* **2014**, *20*, 9627.

[145] R. Konar, G. D. Nessim, *Mater. Adv.* **2022**, *3*, 4471.

[146] R. Konar, . Rosy, I. Perelshtein, E. Teblum, M. Telkhozhayeva, M. Tkachev, J. J. Richter, E. Cattaruzza, A. Pietropolli Charmet, P. Stoppa, M. Noked, G. D. Nessim, *ACS Omega* **2020**, *5*, 19409.

[147] R. Konar, S. Das, E. Teblum, A. Modak, I. Perelshtein, J. J. Richter, A. Schechter, G. D. Nessim, *Electrochim. Acta* **2021**, *370*, 137709.

[148] R. Konar, R. Tamari, E. Teblum, G. D. Nessim, L. Meshi, *Mater. Charact.* **2022**, *184*, 111666.

[149] R. Konar, B. Rajeswaran, A. Paul, E. Teblum, H. Aviv, I. Perelshtein, I. Grinberg, Y. R. Tischler, G. D. Nessim, *ACS Omega* **2022**, *7*, 4121.

[150] C. Zhu, Z. Zeng, H. Li, F. Li, C. Fan, H. Zhang, *J. Am. Chem. Soc.* **2013**, *135*, 5998.

[151] Y. Zhang, B. Zheng, C. Zhu, X. Zhang, C. Tan, H. Li, B. Chen, J. Yang, J. Chen, Y. Huang, L. Wang, H. Zhang, *Adv. Mater.* **2015**, *27*, 935.

[152] R. K. Sen, P. Prabhakar, N. Bisht, M. Patel, S. Mishra, A. K. Yadav, D. V. Venu, G. K. Gupta, P. R. Solanki, S. Ramakrishnan, D. P. Mondal, A. K. Srivastava, N. Dwivedi, C. Dhand, *Curr. Med. Chem.* **2022**, *29*, 5815.

[153] . Kenry, A. Geldert, X. Zhang, H. Zhang, C. T. Lim, *ACS Sens.* **2016**, *1*, 1315.

[154] A. Geldert, . Kenry, X. Zhang, H. Zhang, C. T. Lim, *Analyst* **2017**, *142*, 2570.

[155] S. Su, H. Sun, W. Cao, J. Chao, H. Peng, X. Zuo, L. Yuwen, C. Fan, L. Wang, *ACS Appl. Mater. Interfaces* **2016**, *8*, 6826.

[156] A. Geldert, . Kenry, C. T. Lim, *Sci. Rep.* **2017**, *7*, 17510.

[157] V. S. Chaudhary, D. Kumar, S. Kumar, *IEEE Sens. J.* **2021**, *21*, 17800.

[158] V. S. Chaudhary, D. Kumar, S. Kumar, *IEEE Trans. Plasma Sci.* **2021**, *49*, 3803.

[159] J. Tian, C. Xu, S. Cui, L. Ma, Y. Fu, *Plasmonics* **2021**, *16*, 1451.

[160] M. Rakibul Islam, A. N. M. Iftekher, M. S. Anzum, M. Rahman, S. Siraz, *IEEE Sens. J.* **2022**, *22*, 5628.

[161] D. Zhang, H. Wei, S. Krishnaswamy, *IEEE Photonics Technol. Lett.* **2019**, *31*, 1725.

[162] R. Srivastava, Y. K. Prajapati, S. Pal, S. Kumar, *IEEE Sens. J.* **2022**, *22*, 14834.

[163] A. Shafkat, A. N. Z. Rashed, H. M. El-Hageen, A. M. Alatwi, *J. Sol-Gel Sci. Technol.* **2021**, *98*, 202.

[164] S. Pattnaik, K. Swain, Z. Lin, *J. Mater. Chem. B* **2016**, *4*, 7813.

[165] H. Torkashvand, S. A. Dehdast, M. Nateghpour, A. M. Haghi, G. C. Fard, T. Elmi, M. Shabani, F. Tabatabaie, *Diamond Relat. Mater.* **2023**, *132*, 109670.

[166] G. Figueroa-Miranda, Y. Liang, M. Suranglikar, M. Stadler, N. Samane, M. Tintelott, Y. Lo, J. A. Tanner, X. T. Vu, J. Knoch, S. Ingebrandt, A. Offenhäusser, V. Pachauri, D. Mayer, *Biosens. Bioelectron.* **2022**, *208*, 114219.

[167] P. Jain, S. Das, B. Chakma, P. Goswami, *Anal. Biochem.* **2016**, *514*, 32.

[168] M. T. Hwang, M. Heiranian, Y. Kim, S. You, J. Leem, A. Taqieddin, V. Faramarzi, Y. Jing, I. Park, A. M. van der Zande, *Nat. Commun.* **2020**, *11*, 1543.

[169] A. Panda, P. D. Pukhrambam, *IEEE Trans. NanoBiosci.* **2022**, *21*, 312.

[170] P. Singh, M. Chatterjee, K. Chatterjee, R. K. Arun, N. Chanda, *Sens. Actuators, B* **2021**, *327*, 128860.

[171] M. Nejat, N. Nozhat, *IEEE Sens. J.* **2019**, *19*, 10490.

[172] S. Seyyedmasoumian, A. Attariabad, A. Pourziad, M. Bemani, *IEEE Sens. J.* **2022**, *22*, 14870.

[173] X. Wu, F. Mu, Y. Wang, H. Zhao, *Molecules* **2018**, *23*, 2050.

[174] N. Mohanty, V. Berry, *Nano Lett.* **2008**, *8*, 4469.

[175] H. Qiu, W. Zhou, W. Guo, *ACS Nano* **2021**, *15*, 18848.

[176] F. Haque, J. Li, H.-C. Wu, X.-J. Liang, P. Guo, *Nano today* **2013**, *8*, 56.

[177] J. Hu, W. Lin, B. Lin, K. Wu, H. Fan, Y. Yu, *Ecotoxicol. Environ. Saf.* **2019**, *169*, 370.

[178] A. Barati Farimani, M. Heiranian, K. Min, N. R. Aluru, *J. Phys. Chem. Lett.* **2017**, *8*, 1670.

[179] W. K. Peng, D. Paesani, *J. Pers. Med.* **2019**, *9*, 39.

[180] Y.-F. Fu, Y.-Q. Li, Y.-F. Liu, P. Huang, N. Hu, S.-Y. Fu, *ACS Appl. Mater. Interfaces* **2018**, *10*, 35503.

[181] Q. Zheng, J. Lee, X. Shen, X. Chen, J.-K. Kim, *Mater. Today* **2020**, *36*, 158.

[182] S. Wu, S. Peng, Y. Yu, C. Wang, *Adv. Mater. Technol.* **2020**, *5*, 1900908.

[183] T. T. Tung, M. J. Nine, M. Krebsz, T. Pasinszki, C. J. Coghlan, D. N. Tran, D. Losic, *Adv. Funct. Mater.* **2017**, *27*, 1702891.

[184] L. Xie, X. Zi, Q. Meng, Z. Liu, L. Xu, *Sensors* **2019**, *19*, 1656.

[185] B. Yang, J. Kong, X. Fang, *Nat. Commun.* **2022**, *13*, 3999.

[186] G. Yildiz, M. Bolton-Warberg, F. Awaja, *Acta Biomater.* **2021**, *131*, 62.

[187] A. Hashmi, V. Nayak, K. R. Singh, B. Jain, M. Baid, F. Alexis, A. K. Singh, *Mater. Today Adv.* **2022**, *13*, 100208.

[188] P. Avouris, *Nano Lett.* **2010**, *10*, 4285.

[189] I. Goykhman, U. Sassi, B. Desiatov, N. Mazurski, S. Milana, D. de Fazio, A. Eiden, J. Khurgin, J. Shappir, U. Levy, A. C. Ferrari, *Nano Lett.* **2016**, *16*, 3005.

[190] A. Shashurin, M. Keidar, *J. Phys. D: Appl. Phys.* **2015**, *48*, 314007.

[191] A. G. Cano-Márquez, F. J. Rodríguez-Macías, J. Campos-Delgado, C. G. Espinosa-González, F. Tristán-López, D. Ramírez-González, D. A. Cullen, D. J. Smith, M. Terrones, Y. I. Vega-Cantú, *Nano Lett.* **2009**, *9*, 1527.

[192] P. Zhang, P. He, Y. Zhao, S. Yang, Q. Yu, X. Xie, G. Ding, *Adv. Funct. Mater.* **2022**, *32*, 2202697.

[193] R. Muñoz, C. Gómez-Aleixandre, *Chem. Vap. Deposition* **2013**, *19*, 297.

[194] B. Yu, D. Kuang, S. Liu, C. Liu, T. Zhang, *Sens. Actuators, B* **2014**, *205*, 120.

Raiashree Konar is a joint postdoctoral researcher in Prof. Doron Aurbach's group and Prof. Gilbert Daniel Nessim's group, Chemistry Department, at Bar-Ilan University, Israel. After 3 years of research at CSIR-CGCRI, Kolkata, India, she started her doctoral work (2018–2022) in Prof. Nessim's group on CVD-based syntheses of 2D layered transition-metal dichalcogenides and their alloys, the study of their structural defects, and applications. She currently works on stabilizing high-voltage cathodes in Prof. Aurbach's group and continues her 2D material research in Prof. Nessim's group.

Gilbert Daniel Nessim is an associate professor at Bar Ilan University. His laboratory focuses on the synthesis of 1D and 2D nanostructures using state-of-the-art chemical vapor deposition (CVD) equipment, focusing on better understanding of the complex growth mechanisms of these nanostructures to functionalize and integrate them into innovative devices. He holds a Ph.D. degree in materials science and engineering from MIT, an MBA from INSEAD (France), and a master's degree in electrical engineering from the Politecnico di Milano and the Ecole Centrale Paris. Prior to his Ph.D., he spent a decade in the high-tech industry and consulting across Europe, the USA, and Israel.

Mohamed Belmoubarik is an assistant professor at Mohammed VI Polytechnic University, Morocco. He completed his Ph.D. from Tohoku University, Japan, in 2014, with a specialization in spintronics. He was the first to challenge the fabrication of (111)-oriented magnetic tunnel junctions (MTJs) as an alternative to the conventional (001) MgO–MTJs. He joined NIMS Japan (2015–2017) as a scientific researcher of the development of spinel oxide-based MTJs. At INL, Portugal, he joined several interdisciplinary research projects. He received three competitive grants from JSPS Japan and EU-Horizons 2020, participated in filling three patents, and disseminated his research in peer-reviewed papers (≈20).

Weng Kung Peng is a research group leader at Songshan Lake Materials Laboratory (SSLAB). His research group interest focuses on developing and translating technological innovations (e.g., NMR-based PoCT, machine learning) for rapid "molecular fingerprint." Prior to joining SSLAB, he was a research scientist at the SMART Massachusetts Institute of Technology. He holds several key patents and has first/senior authored several seminal papers that appeared in Nature Medicine, Communications Biology, NPJ Aging and Mechanisms of Disease, NPG Asia Materials, NPJ Science of Food and attracted worldwide press coverage. In 2014, he was listed as one of the "100 Leading Global Thinkers."